ESTIMATION OF DIRECTION OF ARRIVAL (DOA) AND BEAMFORMING USING PLANAR ARRAY

T06391

Fawad Zamaan

140-FET/MSEE/S08

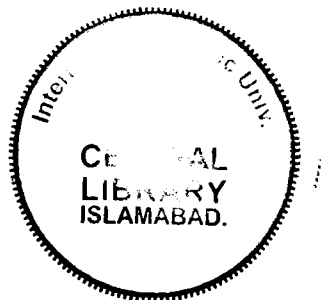MS Electronic Engineering

International Islamic University, Islamabad

August 2009

Tracking radar
Radio direction finders
Antenna arrays
Signal Processing
Electronics in navigation

International Islamic University, Islamabad

<div dir="rtl">

بسم الله الرحمن الرحيم

</div>

In the Name of

ALLAH

Who is the Most Gracious and Merciful

<div dir="rtl">

قالوا سُبْحَانَكَ لا عِلْمَ لَنَا إِلاَّ مَا عَلَّمْتَنَا إِنَّكَ أَنتَ الْعَلِيمُ الْحَكِيمُ

</div>

They said: Be Glorified! we have no knowledge saving that which Thou hast

taught us. Lo! Thou, only Thou, art the Knower the Wise.

[Surah Al-Baqara Verse 32]

Declaration

Certified that the work contained in this thesis entitled

ESTIMATION OF DIRECTION OF ARRIVAL (DOA) AND BEAMFORMING USING PLANAR ARRAY

Is totally my own work and no portion of the work referred in this thesis has been submitted in support of an application for another degree or qualification of this or any other institute of learning.

Fawad Zaman
Reg. No. 140-FET/MSEE/S08

International Islamic University, Islamabad

Certificate of Approval

It is certified that we have read the thesis titled **"Estimation Of Direction Of Arrival (DOA) And Beamforming Using Planar Array"** submitted by **Fawad Zaman, Registration # 140-FET/MSEE/S08** which in our judgment, is of sufficient standard to warrant its acceptance by the International Islamic University, Islamabad for the award of MS in Electronic Engineering degree.
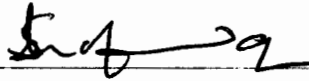
External Examiner

Dr. Muhammad Arif
Professor
Air University, Islamabad.

Internal Examiner

Dr. Muhammad Shafiq
Professor.
Department of Electronic Engineering,
Faculty of Engineering & Technology,
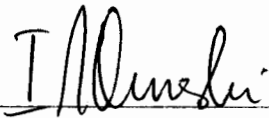International Islamic University, Islamabad.

Co-Supervisor

Dr. Aqdas Naveed Malik
Assistant Professor
Department of Electronic Engineering,
Faculty of Engineering & Technology,
International Islamic University, Islamabad.

Supervisor

Dr. I.M Qureshi
Professor
Air University, Islamabad

Acknowledgements

All Thanks to ALMIGHTY ALLAH, the most gracious and the beneficent, who gave me an opportunity to join the degree course of MS at I.I.U Islamabad and then make me able to complete this work. I express my sincere gratitude to my supervisor, "Dr. I. M. Qureshi" for his continual encouragements and enthusiasm. I never saw a person , who always treated me as his own child and pay special attention to me, studies and my research in all stages. My sincere thanks also goes to my co-supervisor "Dr. A. N. Malik" and "Dr. T. A Cheema" who helped and guided me in completing this thesis.

I am also thankful to my friend "Mr. Kabir Ashraf and Mr. Zafar Ullah Khan" for their timely help and support during my work. I am also indebted to them for their wonderful friendship and helpful advice.

Last but not least I would like to mention the great effort of my family specially my parents who guided and encouraged me throughout my life. I would like to thank my mother for providing me psychological strength to bear the mental stress and hardship during my study and research work. I would also like to mention the special co-operation and encouragement of my younger brother "Mr. Jawad Zaman" during my work.

There is no way, no words, to express my love and gratitude.

Fawad Zaman

Dedicated to My Parents and Siblings

Who always love and pray for my success

Table of Contents

List of Figures

Antenna Related Notation

U_o	Radiation intensity
D	Directivity (Dimensionless)
U	Average Radiation Intensity
L	Dipole Length
d	Spacing Between The Adjacent Elements
Ω_A	Beam Solid Angle
AF	Array Factor
P_{rad}	Power Radiated
Z_A	Antenna Impedance
W	Weight
R_r	Radiation Resistance
$HPBW$	Half Power Beam width
θ	Azimuth Angle
$\emptyset$	Elevation Angle
Z_w	Wave Impedance
β	Progressive Phase Shift
P	Number Of Sources
τ	Propagation Delay
$n_{(t)}$	Noise
R	Correlation Matrix
λ	Wave length

Abbreviations

LOS	Line-Of-Sight
EM	Electromagnetic
SNR	Signal-to-Noise Ratio
DOA	Direction Of Arrival
MUSIC	Multiple Signal Classification
ESPRIT	Estimation Of Signal Parameter Through Rotation Invariant Technique
AF	Array Factor
ULA	Uniform Linear Array
MSE	Mean Square Error
LMS	Least Mean Square
RLS	Recursive Least Square
MVDR	Minimum-Variance Distortion less Response
MIMO	Multi-Input Multi-Output
MMSE	Minimum Mean Square Error
DFT	Discrete Fourier Transform
iid	independent identically distributed
NLOS	Non-Line-Of-Sight

Abstract

This dissertation presents to estimate DOAs and Beamforming by using planar array . It is assumed that the planar array is acting as a radar, so when ever, target is detected then this planar array is able to estimate accurately the angle of arrival by using ESPRIT algorithm and then generate a beam on the same estimated angles at the same time. This work can be divided into three sections.

In the first part, the comparison of DOA for linear array by using MUSIC and ESPRIT algorithm is calculated and it is observed that ESPRIT is more accurate algorithm then MUSIC.

In the second part DOAs are estimated for planar array by using ESPRIT algorithm for different no of elements.

In the last section beam is generated on the same estimated angles of arrival by using planar array. It is also shown that the directivity of planar array improves when the no of elements are increased.

Introduction

1.1 Wireless Communications

The wireless communication is an exciting and challenging area of research in the recent years, which faces the main challenges of (1) increasing data rates while using a limited bandwidth and (2) improving performance while incurring little or no increase in bandwidth or power. As bandwidth available to the service is limited so the designers have to use some techniques to increase the data rate at a given bandwidth. The power requirements issue is also important, that the devices should use as little power as possible to conserve battery life and to keep the products small. The channel in wireless communication is random and unpredictable by its nature and error rates in wireless communication are poorer than that of wired channel.
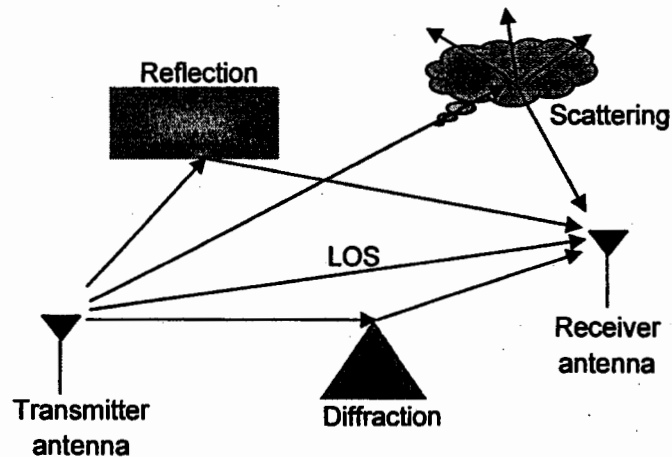
Figure 1.1 Wireless Communications

1.1.1 Multi-paths in Wireless Communications

In wireless communication a major problem is the reception of out-of-phase multi-paths which causes deep attenuation in the received signal. The main reasons of these multi-paths are the scatters in the environment. The scatters in wireless communication acts sometimes as hurdles and sometimes these scatters are used for benefits. The waves from transmitter to receiver adapt various paths due to the different types of hurdles in the environments. Some most common ways in wireless communication are:

- Line of sight (LOS)

- Reflection
- Diffraction
- Scattering

The direct path between the transmitter and the receiver is called the *line-of-sight (LOS)*. The signal receive through the LOS is usually strongest and dominant signal. At least, the signal received through LOS is more deterministic than the reflected receive signal. The LOS does not exist when large objects obstruct the line between the transmitter and the receiver.

Electromagnetic (EM) wave may reflect when it meets an object that is much larger than its wavelength. The wave may reach to the receiver through reflection from many surfaces. The *reflected* waves go through longer distances which results, change in power strengths and phases than those of the LOS path.

When the electromagnetic wave hits a surface with irregularities like sharp edges its path changes and this phenomenon is called *diffraction*.

Scattering phenomena also happens in wireless communication and it occurs when there are a large number of objects smaller than the wavelength between the transmitter and the receiver.

Time variation is also a major problem, which causes due to rapid movement of mobile unit and objects. These problems results signal attenuation which causes decrease in signal-to-noise ratio (SNR). As a result of decrease in SNR, the bit error rate occurs which degrades the performance.

1.1.2 Ways to Improve Performance
Performance of wireless communication can be improved by

- **Increasing Signal to Noise ratio (SNR);**

- **Pre-coding;**

- **Diversity techniques;**

- **Adaptive signal processing algorithms and;**

- **Use of smart/ directional antennas.**

Performance can be improved by increasing SNR which can be done by transmitting signal at high power, but there is a limit on that. This limit is due to safety reason as radio waves are dangerous to human being and also to avoid the interference of other radio signals working on the same frequency.

Performance can also be improved by pre-coding the transmitted signal. By using some coding techniques before transmission, we can recover the erroneously received data.

Diversity techniques are also used for obtaining reliable communication in which the multiple replicas of the transmitted signals are reached at the receiver side under varying fading environment.

We can also improve the performance by exploiting highly complex adaptive algorithms at detectors. These algorithms are usually based on channel estimation. In these algorithms, channels are estimated by transmitting some known bits called *training bits*. These adaptive algorithms update channels information regularly on the basis of error on the receiver side.

Performance can be improved by using the directional smart antennas. Smart antennas generally encompass both switched beam and beam-formed adaptive systems. Switched beam systems have several available fixed beam patterns. A decision is made as to which beam to access, at any given point in time, based upon the requirements of the system. Beam-formed adaptive systems allow the antenna to steer the beam to any direction of interest while simultaneously nulling interfering signals.

1.2 Literature Review

The localization of radiating energy sources by observing their signal received at spatially separated antenna elements is of considerable importance occurring in many fields, including radar, sonar, mobile communication and in other areas. The MUSIC (Multiple Signal Classification) [3] gives a complete geometric solution in the absence of noise, cleverly extending the geometric concepts to obtain a reasonable approximate solution in the presence of noise.

The MUltiple SIgnal Classification (MUSIC) algorithm has received the most attention and has been widely studied in [3]-[6]. Its popularity stems primarily from its generality. Thus to estimate the arrival directions of multipath signals, the MUSIC algorithm [3] and various other methods are being studied for use with resolutions higher , which is the most basic estimation method. The Direction of Arrival (DoA) estimation methods are described in [1-3]. Many DOA estimation algorithms and analytical performance bounds have been developed. Beam-former [7] method which scans the main beam of array antenna is the most fundamental technique. The other techniques based on eigen value decomposition of array input correlation matrix are the Min-Norm method, MUSIC (Multiple Signal Classification) [11], and ESPRIT (Estimation of Signal Parameters via Rotational Invariance Techniques) are discussed in [4,9]

1.3 Scope and Outline of the Work

In this work we used planar arrays for estimation of directional of arrivals (DOA). The directional of arrivals (DOA) estimation (θ, ϕ) for different number

of elements in the x and y direction is also calculated. The effect of number of elements on estimation of directional of arrivals (DOA) is also observed.

We also generate a beam towards the same estimated angles $(\theta, \emptyset)$ for tracking the target.

Thus our system simultaneously calculated the estimated angles $(\theta, \emptyset)$ (directional of arrivals (DOA)) and generated beam towards the target as in case of radar or smart antenna.

1.4 Organization of the Work

A substantial portion of this work, namely Chapters 2-6 focuses on the performance of the planar array. In Chapter 2 and Chapter 3 we present an overview of basic and linear array antennas respectively. Planar arrays are described in chapter 4 and in chapter 5 we discussed direction of arrival (DOA). In chapter 6 we discuss and analyses the results. Chapter 7 concludes the work.

Basic Antenna Concepts

2.1 Antenna Concepts

The radio antenna is the structure associated with the region of transition between a guided wave and a free-space wave. The omni-directional antennas which are known as traditional antennas are not an efficient way to control interferences either it is inter-cell or intra-cell [31]. These types of antennas radiate power in all directions, which is a waste of power. On the other hand one of the cost-effective ways is to split the wireless cell into multiple sectors using sectorized antennas. These types of antennas transmit and receive in a limited portion of a cell, typically one third of circular area, which reduces over all interference in the system [25]. That array uses advanced signal processing algorithms [18] for this purpose that together performs "smart" transmission and reception of signals. The term "smart antenna" generally refers to any antenna array, which can adjust or adapt its own beam pattern in order to emphasize signals of interest and to minimize interfering signals.
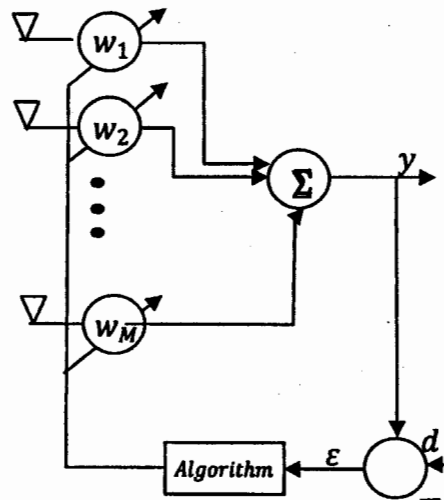
Figure 2.1 smart antenna

2.2 Antennas Gain

The gain of the antennas depends on both its direction and its efficiency. Omni directional antennas radiate equal amounts of power in all directions while directional antennas, on the other hand, have more gain in certain

directions and less in others. The gain of directional antennas in the boresight is more than that of omnidirectional antennas, and is measured with respect to the gain of omnidirectional antennas.

2.3 Radiation Intensity

The power radiated from an antenna per unit solid angle is called the radiation intensity [25]. The general radiation intensity indicates the radiation pattern of the antenna in three dimensions. All isotropic antennas have non-uniform radiation intensity and therefore a non-uniform radiation pattern.

2.4 Directivity

The directivity of an antenna is defined by the ration of the maximum radiation intensity to the average radiation intensity.

If maximum radiation intensity is represented as U_{max} and average radiation intensity as U then the directivity (dimensionless) is represented as

$$D = {U_{max}}/{U} \qquad (2.1)$$

2.5 Beam width

It is defined as the angular separation between two identical points of opposite side of the pattern maximum [26]. Half power beam width (HPBW) is the most widely used beam width as shown in Figure (2.2)
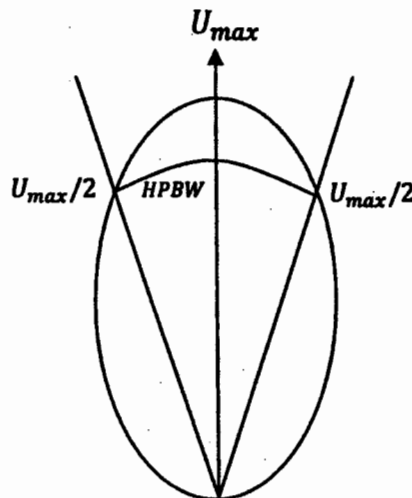
Figure 2.2 The half power beam width

2.6 Antenna Field Regions

Antennas produce complex electromagnetic (EM) fields both near to and far from the antennas. In these field regions some of the fields remain in the vicinity of the antenna and are viewed as reactive near fields; much the same way as an inductor or capacitor is a reactive storage element in lumped element circuits. These field regions are shown in figure 2.3 [1]
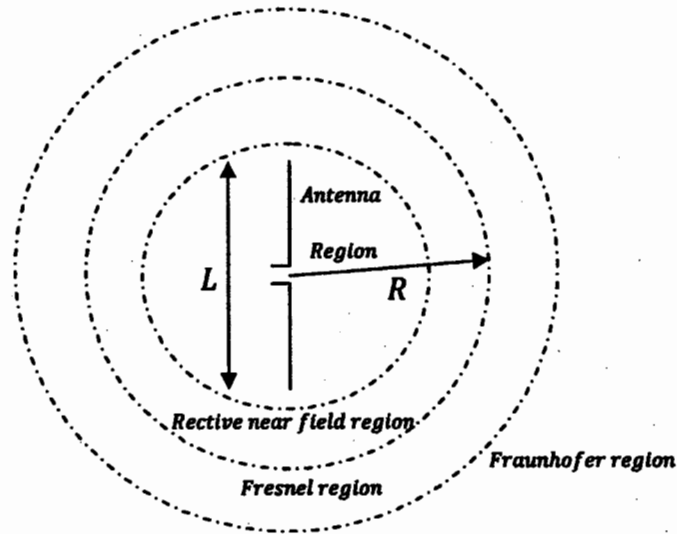
Figure 2.3 Antenna field regions

The different regions and their boundaries are defined as follows:

2.6.1 Antenna region
That region which circumscribes the physical antenna boundaries is called the antenna region as defined by

$$R \leq {}^{L}/_{2} \tag{2.2}$$

2.6.2 Reactive near-field region
That region which contains the reactive energy surrounding the antenna is called the reactive near-field region [1].

$$R \leq 0.62\sqrt{{L^3}/_{\lambda}} \tag{2.3}$$

2.6.3 Fresnel region (radiating near field)
That region which lies between the reactive near-field and the Fraunhofer far field is the Fresnel region or radiating near-field region [28].

$$0.62\sqrt{{L^3}/_{\lambda}} \leq R \leq {2L^2}/_{\lambda} \tag{2.4}$$

2.6.4 Fraunhofer region (far-field)
That region which lies beyond the near- field and where the radiation pattern is unchanging with distance is defined as the Fraunhofer region.

$$R \leq \frac{2L^2}{\lambda} \qquad\qquad (2.5)$$

2.7 Antenna Types

Different antennas are designed according to different requirement. The most important antennas are [29]:

- Dipole Antennas
- Yagi Antennas
- Parabolic Dish antennas
- Slotted Antennas
- Linear array antennas
- Planar Antennas

2.7.1 Dipole antennas

A dipole antennas have a generalized radiation pattern. The elevation pattern shows that a dipole antenna is best used to transmit and receive from the broadside of the antenna. Physically, dipole antennas are cylindrical in nature, and may be tapered or shaped on the outside to conform to some size specification. The antennas are usually fed through an input coming up to the bottom of the antenna but can be fed into the center of the antenna as well.

2.7.2 Yagi Antennas

Yagi antennas consist of an array of independent antenna elements, with only one of the elements driven to transmit electromagnetic waves. The number of elements (specifically, the number of director elements) determines the gain and directivity.
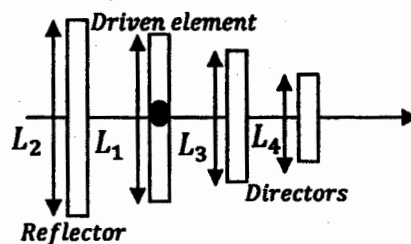
Figure 2.4 Yagi antenna

2.7.3 Slotted antennas

The slotted antenna exhibits radiation characteristics that are very similar to those of the dipole. The elevation and azimuth patterns are similar to those of the dipole, but its physical construction consists only of a narrow slot cut into ground plane.

2.7.4 Linear array antennas

Linear arrays antennas have two or greater than two elements which are aligned along a straight line and generally have a uniform interelement

spacing [20]. Non-uniform linear array antennas are also used according to the requirements. Linear arrays are discussed in chapter 3.

2.7.5 Planar array antennas

Instead of positioning elements along a line ,individual elements can be placed along a rectangular grid to form a rectangular or planar array.Planar arrayas are more versatile and it can give a patteren which is more symmetric and having low side lobes [20]. Moreover planar arrays can be used to scan the main beam of antenna towards any direction in space. Planar arrays are discussed in chapter 4.

3

Linear Array Antennas

3.1 Linear Arrays

In linear arrays all elements are aligned along a straight line and generally have a uniform interelement spacing [20]. The uniform linear arrays are the simplest to analyze and designed. The minimum length in case of linear array is the 2-element array.

3.1.1 Two elements Array

As discussed above that the two elements array is the most fundamental uniform linear array. Let us assume a two element linear array having distance d between them as shown in Figure 3.1[1]
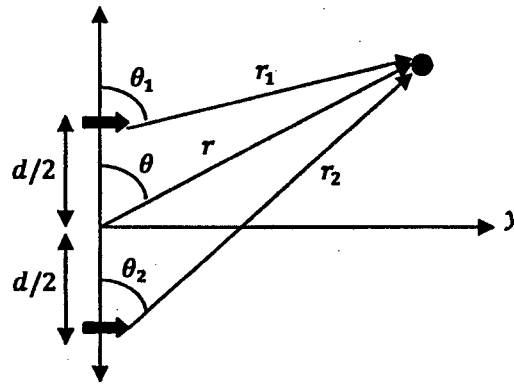
Figure 3.1 The Two infinitesimal dipoles [1]

The field point is located at a distance r from the origin such that $r >> d$.
Thus we assumed the following assumption for phase variation [1]:

$$r_1 \approx r - (^d/_2)cos\theta$$
$$r_2 \approx r + (^d/_2)cos\theta$$
(3.1)

And in case of amplitude variation we assumed:

$$r_1 \approx r_2 \approx r$$
(3.2)

Also we used the assumption [25]

$$\theta_1 \approx \theta_2 \approx \theta$$
(3.3)

Then the above Figure 3.1 will be represented as
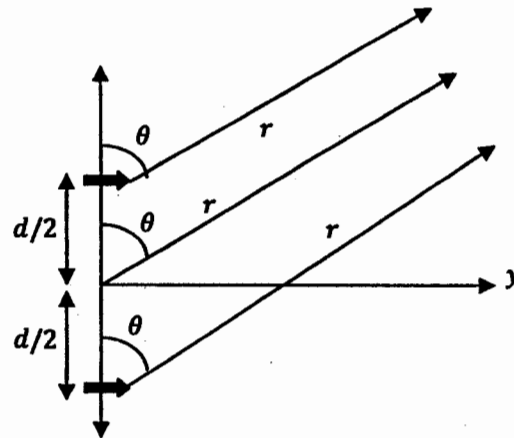
Figure 3.2 The Two infinitesimal dipoles (Far-field observation) [1]

As we know that the total electric field radiated by an array is equal to the sum of the individual element fields, thus in our case of two elements array, the total electric field will be given as

$$E_t = E_1 + E_2$$ (3.4)

Where E_t is the total eclectic field and E_1 and E_2 are the eclectic field of element 1 and element 2.

Thus the total eclectic field E_t will be given as

$$E_t = \frac{jk\eta I_o L e^{-jkr}}{4\pi r} \cos\theta . \left(2\cos\left(\frac{kd\cos\theta + \delta}{2}\right)\right)$$ (3.5)

Where δ = electrical phase difference between the two adjacent elements
L = The dipole length
d = The space between adjacent elements.

The above equation 3.5 can be divided into two parts [20], these parts are:

$$Element\ factor = \frac{jk\eta I_o L e^{-jkr}}{4\pi r} \cos\theta$$ (3.6)

And

$$Array\ factor\ (AF) = \left(2\cos\left(\frac{kd\cos\theta + \delta}{2}\right)\right)$$ (3.7)

The array factor in normalized form $(AF)_n$ is given as

$$Normalized\ array\ factor\ (AF)_n = \cos\left(\frac{kd\cos\theta + \delta}{2}\right)$$ (3.8)

The arrays factor depends on the geometry of the array i-e the elements spacing, phase excitation and the number of elements of the array. It is also notable that each array has its own array factor.

3.1.2 Uniform N-Elements Linear Array

In case of uniform linear array, all the elements are equally spaced and have equal amplitudes as shown in Figure 3.3
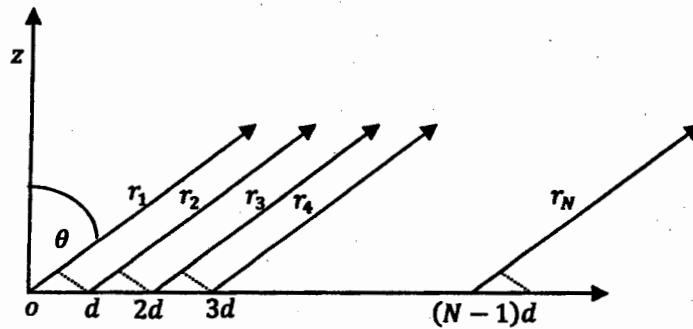
Figure 3.3 N-elements array of isotropic sources [20]

As discussed earlier that each element has its own array factor so in case of N-elements, the array factor is given as

$$Array\ Factor\ (AF) = 1 + e^{j(kdsin\theta+\delta)} + e^{j2(kdsin\theta+\delta)} + \dots + e^{j(N-1)(kdsin\theta+\delta)} \quad (3.9)$$

Or it can also be represented as

$$Array\ Factor\ (AF) = \sum_{n=1}^{N} e^{j(n-1)(kdsin\theta+\delta)} \quad (3.10)$$

If we take new variable ψ as

$$\psi = kdsin\theta + \delta \quad (3.11)$$

Then the above Equation 3.10 can be represented as [20]

$$Array\ Factor\ (AF) = \sum_{n=1}^{N} e^{j(n-1)\psi} \quad (3.12)$$

As each isotropic element has unity amplitude, the entire behavior of this array is dictated by the phase relationship between the elements. The phase is directly proportional to the element spacing in wavelengths.

After applying some mathematical operation [1] we get the simplified form of the array factor as

$$\text{Array Factor (AF)} = \left[\frac{\sin\left(\frac{N}{2}\psi\right)}{\sin\left(\frac{1}{2}\psi\right)}\right] \tag{3.13}$$

The normalized value of AF is given as

$$\text{Array Factor (AF)}_n = \frac{1}{N}\left[\frac{\sin\left(\frac{N}{2}\psi\right)}{\sin\left(\frac{1}{2}\psi\right)}\right] \tag{3.14}$$

This is approximately equal to,

$$\text{Array Factor (AF)}_n \approx \left[\frac{\sin\left(\frac{N}{2}\psi\right)}{\frac{N}{2}\psi}\right] \tag{3.15}$$

The <u>array null</u> occur when the numerator argument of the above equation (3.15) will be

$$\frac{N}{2}\psi = \pm n\pi \tag{3.16}$$

So

$$\theta_{null} = \cos^{-1}\left[\frac{\lambda}{2\pi d}\left(-\beta \pm \frac{2n}{N}\pi\right)\right] \tag{3.17}$$

The <u>array maximum</u> occur when the value of denominator argument of the above equation 3.15 will be

$$\frac{\psi}{2} = 0 \tag{3.18}$$

So

$$\theta_{max} = \cos^{-1}\left(\frac{\lambda\delta}{2\pi d}\right) \tag{3.19}$$

3.1.3 Broadside Array

In case of broadside array all the elements are in phase, so the phase angle $\delta = 0$ in this case [19]. Thus in broadside array the maximum radiation of an array directed normal to the axis of the array and two major lobes are seen because the broadside array is symmetric about the $\theta = \pm\frac{\pi}{2}$ line.

Thus in broadside array the equation (3.15) becomes

$$\psi = kd\cos\theta + \delta = 0 \tag{3.20}$$

As $\theta = \pm\frac{\pi}{2}$ then

$$\psi = kd\cos\theta + \delta|_{\theta=90} = \delta = 0 \tag{3.21}$$

3.1.4 Ordinary End-Fire Array

In end-fire array as name shows the array's maximum radiation is along the axis containing the array elements [1]. For end-fire array we take the value of $\delta = \pm kd$. To direct <u>first maximum towards $\theta = 0^o$</u>

$$\psi = kd\cos\theta + \delta|_{\theta=0} = kd + \delta = 0 \qquad (3.22)$$

or

$$\delta = -kd \qquad (3.23)$$

And towards $\underline{\theta = 180^\circ}$ then

$$\psi = kd\cos\theta + \delta|_{\theta=180} = kd + \delta = 0 \qquad (3.24)$$

or

$$\delta = kd \qquad (3.25)$$

It is notable that mainlobe width for the ordinary end-fire case is much greater than the mainlobe width for the broadside case.

3.2 Array Weighting

As we discussed above the case of linear array having uniform spacing and uniform amplitude. Now we are discussing the case of linear array having uniform spacing and non uniform amplitude.

Even number of elements   *Odd number of elements*
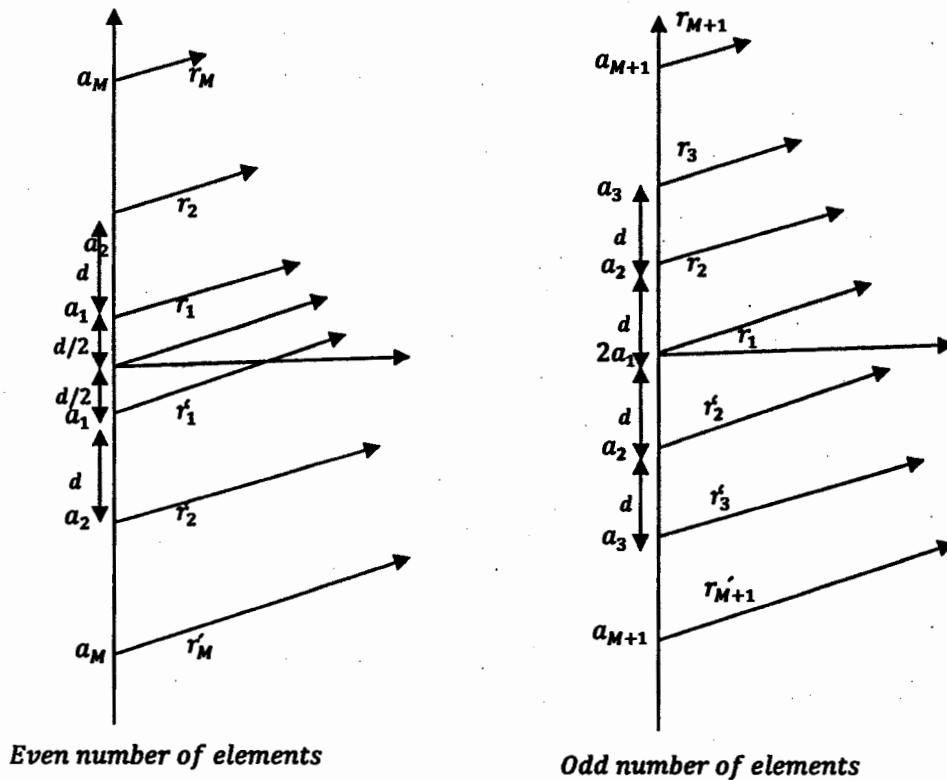
Figure 3.4 Nonuniform amplitude arrays of even and odd number of elements [1]

3.2.1 Array Factor

Consider an even number of elements $2M$ (where M is an integer) are placed symmetrically along the Z − axis [19]. The separation between the elements is d_x and

14

same number of elements are placed along each side of origin as shown in figure (3.6)

$$(AF)_{2M}(even) = \sum_{n=1}^{M} w_n \cos[(2n-1)u] \qquad (3.26)$$

$$(AF)_{2M}(odd) = \sum_{n=1}^{M+1} w_n \cos[(2n-1)u] \qquad (3.27)$$

Where

$$u = \frac{\pi d}{\lambda}\cos\theta$$

The above excitation Co-efficient w_n which is also called weights, can be calculated by using different methods, one of which is Binomial method. By using Binomial expansion J.S Stone suggested that the function $(1+x)^{m-1}$ can be written in a series by using the Binomial expansion, as

$$(1+x)^{m-1} = 1 + (m-1)x + \frac{(m-1)(m-2)}{2!}x^2 + \cdots \qquad (3.28)$$

m=1						1					
m=2					1		1				
m=3				1		2		1			
m=4			1		3		3		1		
m=5		1		4		6		4		1	
m=6	1		5		10		10		5		1
m=7	1	6		15		20		15		6	1

m=8   1   7   21   35   21   35   7   1
m=9 1 8 28   56   70   56   28   8   1
m=10 1 9 36   84   126   126   84   36   9   1

$$(3.29)$$

The above triangle is called Pascal's triangle. If m represents the number of elements of the array, then the coefficients of the expansion represent the relative amplitudes of the elements [27].

From the equation (3.26), (3.27) and (3.29) the amplitude coefficients for the following arrays are:

1. Two elements ($2M = 2$)

$$w_1 = 1$$

2. Three elements ($2M + 1 = 3$)

$$2w_1 = 2$$

$$w_1 = 1$$

and

$$w_2 = 1$$

3. Four elements $(2M = 4)$

$$w_1 = 3$$

and

$$w_2 = 1$$

4. Five elements $(2M + 1 = 5)$

$$2w_1 = 6$$

$$w_1 = 3$$

$$w_2 = 4$$

and

$$w_3 = 1$$

4

Planar Array Antennas

4.1 Planar Array

We consider a planar array with *M* elements in the x-direction and *N* elements in the y-direction creating an $M \times N$ array of elements [1] as shown in Figure 4.1
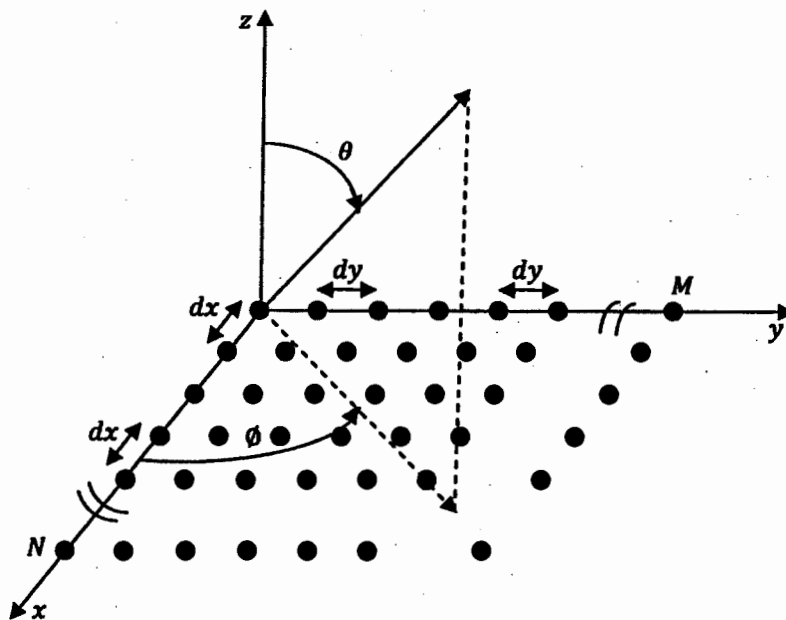
Figure 4.1 Planar array with dimension *M x N* [1]

The x-directed elements are spaced dx apart and the y-directed elements are spaced dy apart. We can view planar array as M linear arrays of N elements or as N linear arrays of M elements [20].

The array factor of this array is given as

$$Total\ Array\ Factor\ (AF) = AF_x . AF_y \qquad (4.1)$$

The array factor along x-direction will be [1]

$$AF_x = \sum_{m=1}^{M} I_{m1} e^{j(m-1)(kd_x \sin\theta\cos\emptyset + \delta_x)} \tag{4.2}$$

And the array factor along y-direction can be represented as

$$AF_y = \sum_{n=1}^{N} I_{1n} e^{j(n-1)(kd_y \sin\theta\sin\emptyset + \delta_y)} \tag{4.3}$$

If we put the value of AF_x and AF_y in equation (4.1) and simplified them (we assume the amplitude excitation of the planar array is constant i-e I_{m1} and I_{1n} are equal to I_o) then the array factor can be written as

$$AF = I_o \sum_{m=1}^{M} e^{j(m-1)(kd_x \sin\theta\cos\emptyset + \delta_x)} \sum_{n=1}^{N} I_{1n} e^{j(n-1)(kd_y \sin\theta\sin\emptyset + \delta_y)} \tag{4.4}$$

If we simplify the above equations and normalized the results, we get

$$AF_n(\theta,\emptyset) = \left[\frac{1}{M}\frac{\sin\left(\frac{M}{2}\varsigma_x\right)}{\sin\left(\frac{\varsigma_x}{2}\right)}\right]\left[\frac{1}{N}\frac{\sin\left(\frac{N}{2}\varsigma_x\right)}{\sin\left(\frac{\varsigma_x}{2}\right)}\right] \tag{4.5}$$

Where

$$\varsigma_x = kd_x \sin\theta\cos\emptyset + \delta_x \tag{4.6}$$

$$\varsigma_y = kd_y \sin\theta\sin\emptyset + \delta_y \tag{4.7}$$

It is also notable that the spacing between the elements plays an important role in the generation of its pattern.

When the spacing between the elements along x-axis and along y-axis is equal or greater than $\lambda/2$, the multiple maxima of equal magnitude are formed. The principle maximum is called as major lobe and others are called grating lobes.

Whereas when the spacing between the elements along x-axis and along y-axis is less than $\lambda/2$ then no grating lobes are formed.

For rectangular planar array, the value of major lobes and corresponding grating lobes are located at [1]

$$kd_x \sin\theta\cos\emptyset + \delta_x = \pm 2m\pi \tag{4.8}$$

$$kd_y \sin\theta\sin\emptyset + \delta_y = \pm 2n\pi \tag{4.9}$$

Where

$$m = 0,1,2,\dots$$

$$n = 0,1,2, \dots$$

The principle maximum is calculated with $m = 0, n = 0$ and the grating lobes can be calculated as

$$kd_x(\sin\theta\cos\emptyset - \sin\theta_o\cos\emptyset_o) = \pm 2m\pi \tag{4.10}$$

$$kd_y(\sin\theta\sin\emptyset - \sin\theta_o\sin\emptyset_o) = \pm 2n\pi \tag{4.11}$$

Where

$$m = 0,1,2, \dots$$
$$n = 0,1,2, \dots$$

When we solve above equations (4.10) and (4.11) for value of $\emptyset$ and θ, and simplify the results we get [1]

$$\emptyset = \tan^{-1}\left[\frac{\sin\theta_o\sin\emptyset_o \pm {n\lambda}/{d_y}}{\sin\theta_o\cos\emptyset_o \pm {m\lambda}/{d_x}}\right] \tag{4.12}$$

And the value of θ is

$$\theta = \sin^{-1}\left[\frac{\sin\theta_o\sin\emptyset_o \pm {n\lambda}/{d_y}}{\sin\phi}\right] \tag{4.13}$$

Or

$$\theta = \sin^{-1}\left[\frac{\sin\theta_o\cos\emptyset_o \pm {m\lambda}/{d_x}}{\cos\phi}\right] \tag{4.14}$$

These above equations for θ and ϕ must be satisfied simultaneously for true grating lobes.

4.1.1 Directivity

The directivity of the array factor can be calculated for the major beam pointing towards angles $\theta = \theta_o$ and $\emptyset = \emptyset_o$ direction as [24]

$$D_o = \frac{4\pi[AF(\theta_o, \emptyset_o)][AF(\theta_o, \emptyset_o)]^*|_{max}}{\int_0^{2\pi}\int_0^{\pi}[AF(\theta, \emptyset)][AF(\theta, \emptyset)]^*\sin\theta d\theta d\emptyset} \tag{4.15}$$

The above equation can be simplified by the most practical case as [1]

$$D_o = \frac{\pi^2}{\Omega_A(\text{rads}^2)} = \frac{32400}{\Omega_A(\text{degrees}^2)} \tag{4.16}$$

Where Ω_A is represents in square radians or square degrees.

5 Signal Modal for Array Processing

5.1 Overview of Directional Of Arrival (DOA)

To understand the concept of Direction of arrival (DOA) and Beamforming, let us relate this issue to human body. Imagine that two persons are involved in conversation inside a dark room. The listener among them can determine the location of the speaker because the voice arrives to the listener ears at different time. So he senses the voice by using his ears and then the human brain determines the location of the speaker. In the mean time if an unwanted speaker also joins the conversation, the listener tries to reject the unwanted speakers voice and concentrate to tune the first speaker voice. Similarly the listener can respond back to the same direction of the desired speaker by orienting the transmitter (mouth) toward the speaker [1]. This is shown in below figure 5.1

Smart antenna system uses exactly the same analogy. It uses antenna elements instead of human ears to sense the information. To locates the direction of the source and to generate the beam towards the desired direction, it uses digital signal processor (DSP) instead of human brains.

The directional of arrival plays an important role for steering the radiation in a particular direction and creation of nulls in the interference direction. It computes the direction of arrivals of all the incoming signals by using some algorithms.
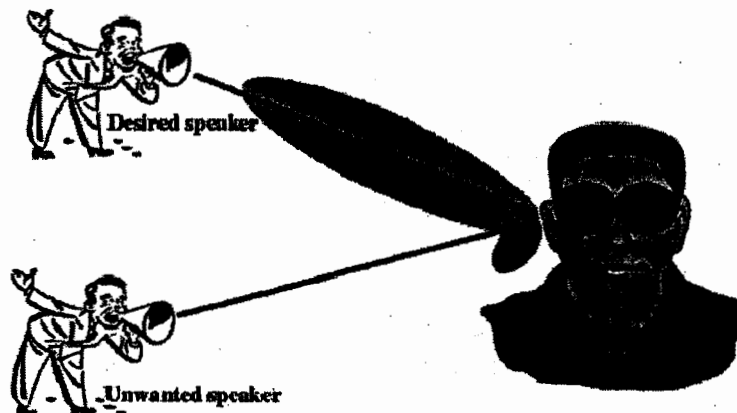
(a) The human analogy [1]
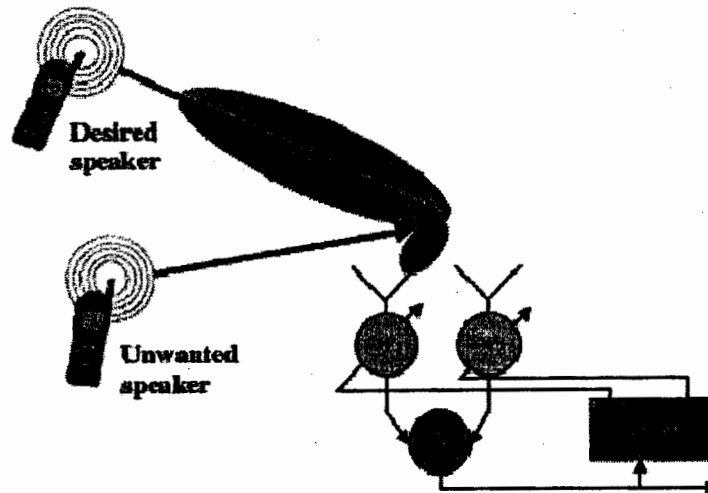
(b) Electrical equivalent [1]

Figure 5.1 The analogy of Smart-antenna and human body

5.1.1 Directional Of Arrival (DOA) Techniques

DOA estimation techniques can be categorized on the basis of the data analysis and implementation into four different areas:

- Conventional methods
- Subspace-based methods
- Maximum likelihood methods
- Integration methods

In case of *Conventional methods* [16] for DOA estimation, we used the concepts of beamforming and null steering and do not focus on the statistics of the received signal. The DOA of all the signals is determined from the peaks of the output power spectrum obtained from steering the beam in all possible directions. Examples of these techniques are delay-and-sum method [7] but this method have poor resolution disadvantage.

The *subspace methods* [19] utilize the structure of the received data, which results in a dramatic improvement in resolution. Examples of this method are the *MUltiple SIgnal Classification (MUSIC)* [13] algorithm and the *Estimation of Signal Parameters via Rotational Invariance Technique (ESPRIT)* [9].

In *Maximum Likelihood (ML)* [22] techniques is considered as the first techniques used for DOA estimation and are less popular than suboptimal subspace techniques because ML methods are computationally rigorous.

The *integrated technique* [23] that combines of two methods, the property-restoral method and the subspace-based approach. The subspace-based mehods as discussed above combines with property-restoral technique that is a Iterative Least Squares Projection Based Constant Modulus Algorithm (ILSP-CMA), a data-efficient

and cost-efficient approach used to detect the envelope of the received signals and overcome many of the problems associated with some old techniques.

5.2 System model for Linear Array

Consider a beamformer of N-elements linear array with arbitrary locations and directional characterizes [19]. The output $y(t)$ of the array with weights w_m is the sum of the received signals $s_k(t)$ and the noise $n(t)$ at the receiver connected to each elements.
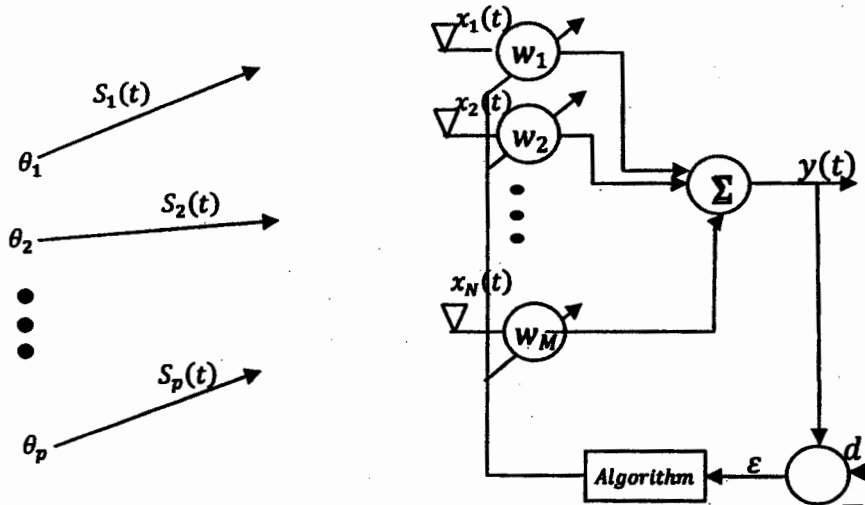
Figure 5.2 The N-elements array with arriving signals

The output of the beamformer is

$$y(t) = w^H x(t) \tag{5.1}$$

Where w is the total output of all weight w_m and w^H is the complex conjugate transpose of the weight vector w. The output of the kth element of the array can be represented as

$$x_k(t) = \sum_{i=1}^{p} a_k(\theta_i) s_i(t - \tau_k(\theta_i)) + n_k(t) \tag{5.2}$$

$$x_k(t) = \sum_{i=1}^{p} a_k(\theta_i) s_i(t) e^{-jw_o \tau_k(\theta_i)} + n_k(t) \tag{5.3}$$

Where p is the narrowband sources with known frequency w_o, $\tau_k(\theta_i)$ is the propagation delay between a reference point and kth antenna element for ith wave front, $a_k(\theta_i)$ is the corresponding elements complex response and $n_k(t)$ is the kth element noise. If the transmitters are moving, the matrix of steering vectors is changing with time and the corresponding arrival angles are changing. The $x(t)$ can be expanded in matrix form as

$$x(t) = \left[a_k(\theta_1), a_k(\theta_2), \ldots, a_k(\theta_p)\right] \begin{bmatrix} s_1(t) \\ s_2(t) \\ \vdots \\ s_p(t) \end{bmatrix} + n_k(t) \qquad (5.4a)$$

$$x(t) = As(t) + n(t) \qquad (5.4b)$$

Here each of the p - complex signals arrives at angles θ_i and is intercepted by the N antenna elements.

5.3 Sytem model for Planar array

Consider antenna array receives the incoming signals from all directions, the DOA algorithm determines the directions of all incoming signals based on the time delays [1].
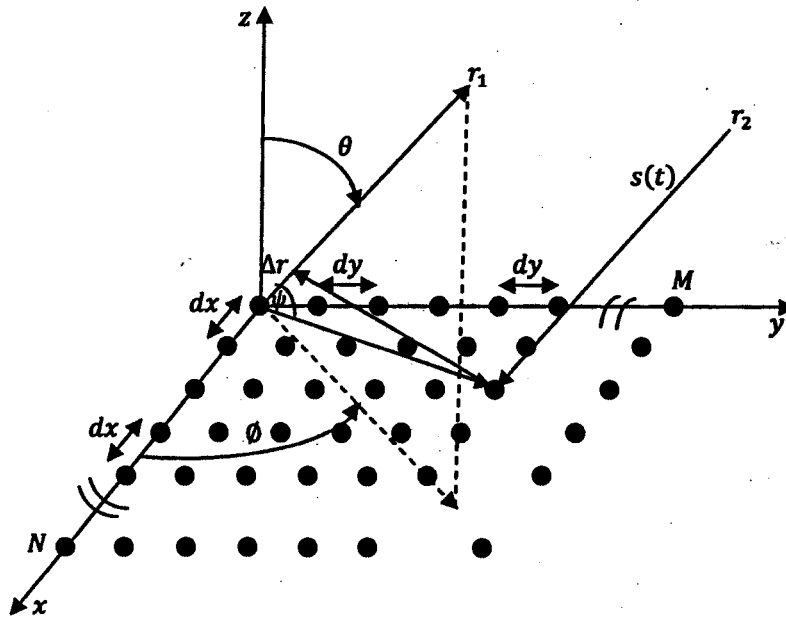
Figure 5.3 The M x N-elements array with graphical representation of time delay [1]

When an incoming wave, carrying a baseband signal s(t) impinges at an angle (θ, ϕ) on the antenna array, it produces time delays relative to the other antenna elements as shown in Figure (5.2)

The time delay of the signal s(t) at the $(m,n)th$ element, relative to the reference element $(0,0)th$ at the origin is given as [1]

$$\tau_{m,n} = \frac{\Delta r}{c} \qquad (5.5)$$

Where Δr is the differential distance and c is the speed of the light in free-space.

The value of Δr is given as

23

$$\Delta r = d_{mn} \cos(\psi) \tag{5.6}$$

Where the distance from the origin to the $(m, n)th$ element is given as

$$d_{mn} = \sqrt{m^2 d_x^2 + n^2 d_y^2} \tag{5.7}$$

and

$$\cos(\psi) = \frac{\hat{a}_r \cdot \hat{a}_\rho}{|\hat{a}_r| |\hat{a}_\rho|} \tag{5.8}$$

Where $\hat{a}_r$ and $\hat{a}_\rho$ are the unit vectors along the direction of the incoming signal s(t) and along the distance d_{mn} to the (m, n)th element respectively.

Now the time delay $\tau_{m,n}$ of the (m, n)th element, with respect to the element at the origin $(0, 0)$th can be represented as

$$\tau_{m,n} = \frac{m d_x \sin\theta\cos\emptyset + n d_y \sin\theta\sin\emptyset}{c} \tag{5.9}$$

5.4 Multiple Signal Classification (MUSIC) Algorithm

Music Algorithm is an extension of Pisarenko Harmonic Decomposition (PHD) [16] method and was presented by Schmitt in 1979. Let us assume that x(t) is a sum of p narrow band non-coherent plane wave signals in white noise and that the number of sources, p generating these signals is known. Let   an N x N estimate of the autocorrelation matrix of $x(t)$ with N $> p + 1$ (In PHD method $N = p + 1$). If the eigenvalues of R_x are arranged in descending order, $q_1, \geq q_2, \geq q_3, \geq ....,q_N$ and if $\{\hat{e}_1, \hat{e}_2, ..., \hat{e}_p, \hat{e}_{p+1}, ..., \hat{e}_N\}$ are the corresponding eigenvectors, then these eigenvectors may be divided into two groups, the p signal plus noise eigenvectors corresponding to p largest eigenvalues and the $N - p$ noise eigenvectors corresponding to the $N - p$ smallest eigenvalues that ideally are equal to σ^2. These $N - p$ noise eigenvectors will be approximately orthogonal to the p steering vectors $a(\theta)$, i.e.

$$a^H(\theta_i) \, \hat{e}_k = 0 \, for \qquad i = 1, 2, ..., p \tag{5.10}$$

$$k = p + 1, ..., N$$

Or simply

24

$$a^H(\theta_i)\,\hat{e}_k = 0 \qquad\qquad for\ k = p + 1,\ldots\ldots,N \qquad (5.11)$$

where $\hat{e}_k$ represents the kth noise eigenvector.
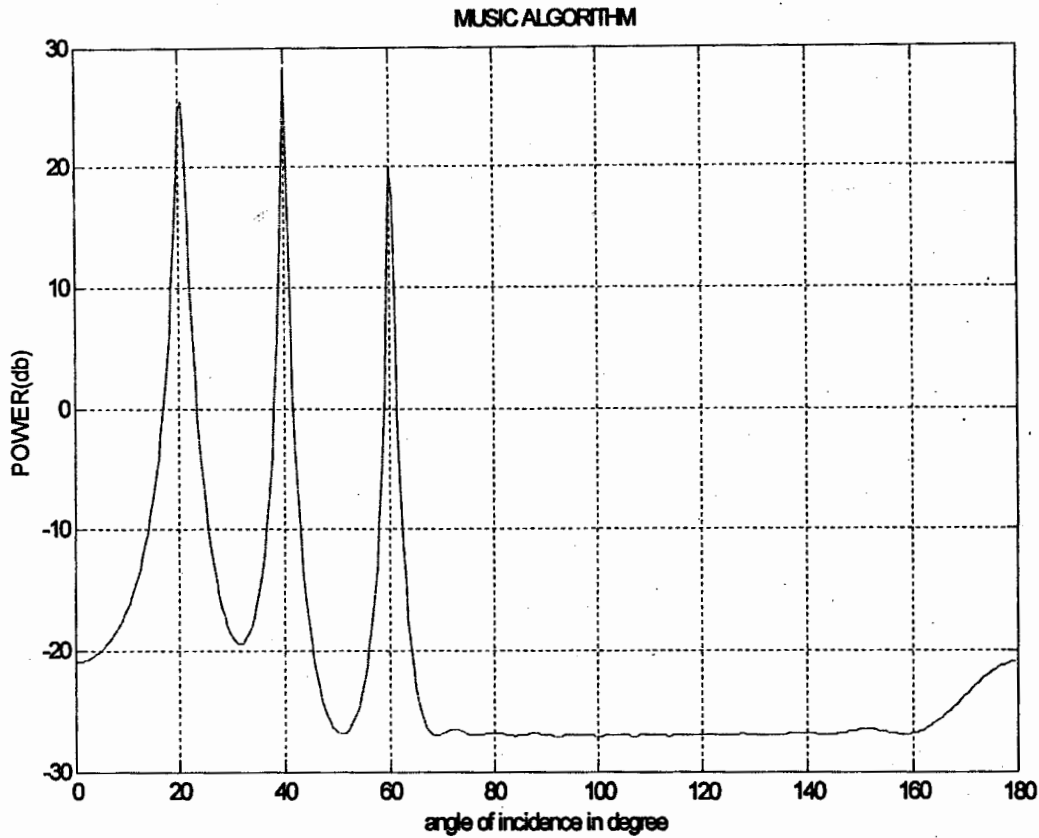
Figure 5.4 Music pseudo spectrums for $\theta_1 = 20^o, \theta_2 = 40^o, \theta_3 = 60^o$

All the $N - p$ noise eigenvectors will share the same p roots. However, because each noise eigenvector is a length N vector, there is an additional $N - p$ roots that are due entirely to the noise i.e each of the noise eigenvector will have these roots due to noise only and that also at random frequencies. This may give rise to the spurious peaks in the pseudo spectrum of single noise eigenvector (as in the case of PHD method.) Therefore when only one noise eigen vector is used to estimate DOA's, there may be some ambiguity in distinguishing the desired peaks from the spurious ones. In MUSIC algorithm the effects of these spurious peaks are reduced by averaging the pseudo spectra obtained for each of the noise eigenvectors i.e. MUSIC algorithm assumes the following form of the DEF or pseudo spectrum.

$$P_{MUSIC}(\theta) = \frac{1}{\sum_{k=p+1}^{N}|a^H(\theta)\hat{e}_k|^2} \tag{5.12}$$

Above equation can be written as

$$P_{MUSIC}(\theta) = \frac{1}{\sum_{k=p+1}^{N}(a^H(\theta)\hat{e}_k)\left(\hat{e}_k^{\ H}a(\theta)\right)} \tag{5.13}$$

Let us define

$$\hat{U}_N = \sum_{k=p+1}^{N}(\hat{e}_k)(\hat{e}_k^{\ H})) \tag{5.14}$$

Then the above Equation 5.13 can be written in amore compact form as follows

$$P_{MUSIC}(\theta) = \frac{1}{a^H(\theta)\hat{U}_N a(\theta)} \tag{5.15}$$

This is called MUSIC pseudo-spectrum. One note able thing about this spectrum is that, it is based on single realization of the stochastic process represented by the snap shots $x(t)$ for $t = 1,2,\ldots\ldots\ldots,M$. Music estimates are consistent and converge to true source bearings as the number of snapshots grows to infinity. However this is true only for the case of uncorrelated signal. For strongly correlated signals, the estimates provided by the MUSIC pseudo spectrum are extremely poor compared with the situation where uncorrelated signals are used. This is the major problem with the music algorithm.

5.5 Multiple Signal Classification (MUSIC) Algorithm for Planar Array

We consider the signal s(t) of the receive signals on the planar array (Figure 5.3) which is represented as [11]

$$s(t) = [s_1(t), s_2(t), \ldots, s_m(t), \ldots, s_M(t)]^T \tag{5.16}$$

The direction vector on the planar array, the direction vectors of the linear arrays in the column direction are first obtained. For the mth arrival signal, the directional vector at column n_2 is given as

$$a_{n_2(\theta_m,\phi_m)} = \left[a_{1,n_2(\theta_m,\phi_m)}, a_{2,n_2(\theta_m,\phi_m)},\ldots,a_{N_1,n_2(\theta_m,\phi_m)}\right]^T \tag{5.17}$$

Which is also given as

$$a_{n_2(\theta_m,\phi_m)} = g_{(\theta_m,\phi_m)}\left[e^{j\delta_{1,n_2}(m)}, e^{j\delta_{2,n_2}(m)}, \ldots, e^{j\delta_{N_1,n_2}(m)}\right]^T \tag{5.18}$$

26

Where $g_{(\theta_m, \emptyset_m)}$ is the directivity gain of an antenna element at the arrival angles θ_m , and $\emptyset_m$.

Similarly the direction vector for planar array is defined as

$$a(\theta_m, \emptyset_m) = \left[a_{1(\theta_m, \emptyset_m)}, a_{2(\theta_m, \emptyset_m)}, ..., a_{N_1(\theta_m, \emptyset_m)} \right]^T \qquad (5.19)$$

The direction of arrival for M arrival signals, having *M x N* planar array is defined as [11]

$$A = [a(\theta_1, \emptyset_1), (\theta_1, \emptyset_1), ..., (\theta_m, \emptyset_m), ..., (\theta_M, \emptyset_M)] \qquad (5.20)$$
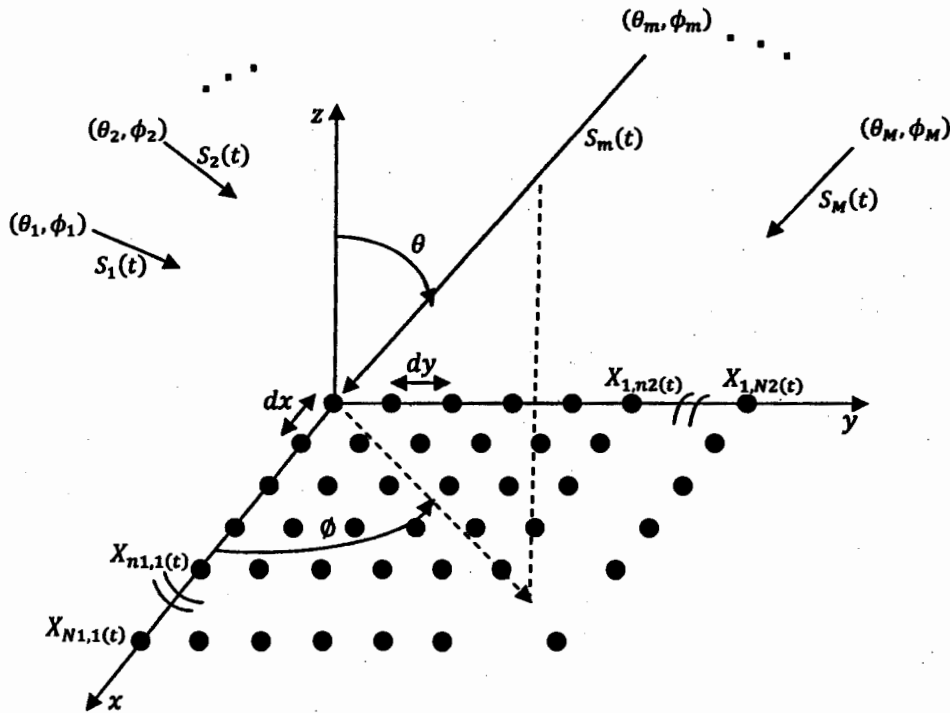
Figure 5.5 Planar Array Geometry for multiple sources DOA estimations using MUSIC

Then the output vector $x(t)$ of the planar array can be expressed as follows

$$x(t) = As(t) + n(t) \qquad (5.21)$$

Where $n(t)$ is an N-dimensional column vector, which denotes internal noise.

The covariance matrix of $x(t)$ can be expressed by the N x N matrix R as follows:

$$R = E\{x(t).x(t)^H\} \qquad (5.22a)$$

$$= APA^H + \sigma^2 I \qquad (5.22b)$$

The eigen values of the covariance matrix R and its corresponding unique eigen vector are λ_i and e_i where $= 1,2,3, \dots N$.

Let $\lambda_1 \geq \lambda_2 \dots \geq e_{M+1} \geq e_{M+2} \geq \dots \geq e_N = \delta^2$. The number of arrival signal can be estimated from λ_M . Due to the property in which the noise subspace spanned by E_N Is orthogonal to the direction vector of the arrival signal, the arrival angles can estimated with the following function [27].

$$P_{MUSIC}(\theta, \emptyset) = \frac{a^H(\theta, \emptyset). a(\theta, \emptyset)}{a^H(\theta, \emptyset)E_N E_N{}^H a(\theta, \emptyset)} \qquad (5.23)$$

5.6 Estimation of Signal Parameters via Rotational Invariance Technique (ESPRIT) Algorithm for Linear Array

The goal of the ESPRIT techniques is to exploit the rotational invariance in the signal subspace which is created by two arrays with a translational invariance structure. ESPRIT inherently assumes narrowband signals so that one knows the translational phase relationship between the multiple arrays to be used [4]. As with MUSIC, [3] ESPRIT assumes that there are $p < N$ narrow-band sources centered at the center frequency f_o . These signal sources are assumed to be of a sufficient range so that the incident propagating field is approximately planar. The sources can be either random or deterministic and the noise is assumed to be random with zero-mean. ESPRIT assumes multiple identical arrays called *doublets*. An example is shown in Figure 5.5 where a six element linear array is composed of two identical doublets. The distance between two elements of the same doublets is d.
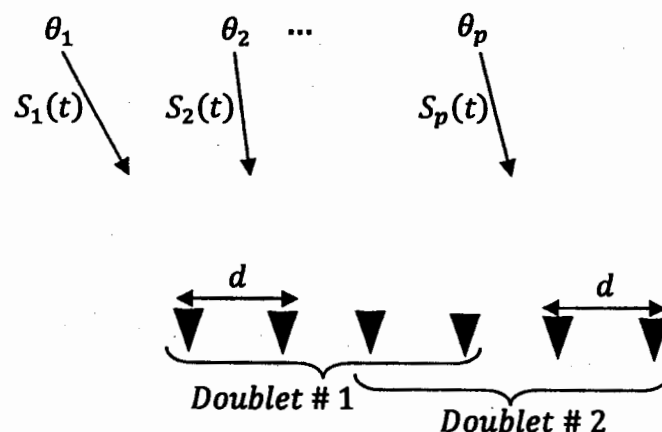

Figure 5.6 Array Geometry for multiple sources DOA estimations using ESPRIT

Let us label these arrays as array 1 and array 2

$$x_1(k) = [a_1(\theta_1), a_1(\theta_2), \dots a_1(\theta_p)] . \begin{bmatrix} s_1(k) \\ s_2(k) \\ . \\ . \\ . \\ s_p(k) \end{bmatrix} + n_1(k) \tag{5.24}$$

$$= A_2.s(k) + n_2(k) \tag{5.25}$$

And

$$x_2(k) = A_1.s(k) + n_1(k) \tag{5.26}$$

$$= A_1 \Phi s(k) + n_2(k)$$

Where

$$\Phi = diag\left\{ e^{jkd\sin\theta 1}, e^{jkd\sin\theta 2} \dots\dots\dots, e^{jkd\sin\theta p} \right\} \tag{5.27}$$

The complete received signal considering the contributions of both sub arrays is give

$$x(k) = \begin{bmatrix} x_1(k) \\ x_2(k) \end{bmatrix} = \begin{bmatrix} A_1 \\ A_1.\varphi \end{bmatrix} s(k) + \begin{bmatrix} n_1(k) \\ n_2(k) \end{bmatrix} \tag{5.28}$$

We can now calculate the correlation matrix for either the complete array or for the two sub-arrays. The correlation matrix for the complete array is given by

$$R_{xx} = E[x.x^H] = AR_{SS} A^H + \sigma^2 I \tag{5.29}$$

Whereas the correlation matrices for the two subarrays are given by

$$R_{11} = E[x_1.x_1{}^H] = AR_{SS} A^H + \sigma^2 I \tag{5.30}$$

And

$$R_{22} = E[x_2.x_2{}^H] = AR_{SS} A^H + \sigma^2 I \tag{5.31}$$

Each of the full rank correlation matrices given in Equation (5.30) and Equation (5.31) has a set of eigenvectors corresponding to the p signals present [12]. Creating the signal subspace for the two subarrays results in the two matrices E_1 and E_2.

Creating the signal subspace for the entire array results in one signal subspace given by E_X. Because of the invariance structure of the array, E_X can be decomposed into the subspaces E_1 and E_2 which are composed of the P eigenvectors corresponding to the largest eigen-values of R_{11} and R_{22} . Since the arrays are translationally related, the subspaces of eigenvectors are related by a unique non-singular transformation matrix such that

$$E_1 \Psi = E_2 \tag{5.32}$$

There must also exist a unique non-singular transformation matrix T Such that

$$E_1 = AT \tag{5.33}$$

$$E_2 = A\phi T \tag{5.34}$$

By substituting Equation 5.33 and Equation 5.34 into Equation 5.32 and assuming that A is of full-rank, we can derive the relationship

$$T\Psi T^{-1} = \phi \tag{5.35}$$

Thus, the eigenvalues of Ψ must be equal to the diagonal elements of ϕ and the columns of T must be the eigenvectors of Ψ. Ψ is a rotation operator that maps the signal subspace E_1 into the signal subspace E_2.

Step for calculating Ψ and its eigenvalues as follow

- Estimate the array correlation matrices R_{11} , R_{22} from the data samples.
- Knowing the array correlation matrices for both sub-arrays, one can estimate the total number of sources by the number of large eigenvalues in either R_{11} or R_{22}
- Calculate the signal subspaces E_1 and E_2 based upon the signal eigenvectors of R_{11} and R_{22}.
- Form *2P x 2P* matrix using the signal subspaces such that

$$C = \begin{bmatrix} E_1{}^H \\ E_2{}^H \end{bmatrix} [E_1 \quad E_2] = E_c \Lambda E_c{}^H \tag{5.36a}$$

Where the matrix E_c is from the eigenvalue decomposition (EVD) of C.
- Partition E_c into four *P x P* sub-matrices such that

$$E_c = \begin{bmatrix} E_{11} & E_{12} \\ E_{21} & E_{22} \end{bmatrix}$$

(5.36b)

- **Estimate the rotation operator**

$$\Psi = -E_{12} E_{22}^{-1}$$

(5.37)

- The eigen-values of Ψ are $\lambda_1, \lambda_2, \ldots, \lambda p$.
- The estimate the angles of arrival (for p number of arrival signal) is

$$\theta_i = sin^{-1}\left(\frac{arg(\lambda_i)}{kd}\right)$$

(5.38)

Where $i = 1,2,3, \ldots, p$

5.7 Estimation of Signal Parameters via Rotational Invariance Technique (ESPRIT) Algorithm for Planar Array

Consider three arrays of sensors located on the x y-plane at the positions $(x_{xi}, y_{yi}), (x_{xi} + u_y, y_{yi} + v_y)$ and $(x_{xi} + u_z, y_{yi} + v_z)$ respectively, where $1 \le i \le N$ [6]

Let there be P narrow-band sources with center frequency ω_o emitting plane wave signals $S_k(t)$, such that the k source has an elevation angle θ_k and azimuth angle $\emptyset_k$[6]. The observed signal at the sensor are [6]

$$x_i(t) = \sum_{k=1}^{p} e^{j\omega_o(\tau,(\theta_i,\emptyset_i))} s_k(t) + n_{x,i(t)}$$

(5.39)

$$y_i(t) = \sum_{k=1}^{p} e^{j\omega_o(T,(\theta_i,\emptyset_i))} e^{j\omega_o(\tau,(\theta_i,\emptyset_i))} s_k(t) + n_{y,i(t)}$$

(5.40)

$$z_i(t) = \sum_{k=1}^{p} e^{j\omega_o(T,(\theta_i,\emptyset_i))} e^{j\omega_o(\tau,(\theta_i,\emptyset_i))} s_k(t) + n_{z,i(t)}$$

(5.41)

Where

$$\tau_i(\theta, \emptyset) = \frac{(x_{xi}\cos\emptyset\sin\theta + y_{yi}\sin\emptyset\sin\theta)}{c} \qquad 1 \le i \le N$$

(5.42)

$$T_k(\theta, \emptyset) = \frac{(u_k\cos\emptyset\sin\theta + v_k\sin\emptyset\sin\theta)}{c} \qquad k = y,z$$

(5.43)

These equations can be represented in matrix form as [6]

$$x(t) = AS(t) + n_x(t)$$

(5.44)

31

$$y(t) = A\emptyset_y S(t) + n_y(t) \tag{5.45}$$

$$z(t) = A\emptyset_z S(t) + n_z(t) \tag{5.46}$$

Where

$$x(t) = [x_1(t), x_2(t), \dots, x_N(t)]^T \tag{5.47}$$

$$y(t) = [y_1(t), y_2(t), \dots, y_N(t)]^T \tag{5.48}$$

$$z(t) = [z_1(t), z_2(t), \dots, z_N(t)]^T \tag{5.49}$$

$$s(t) = [s_1(t), s_2(t), \dots, s_p(t)]^T \tag{5.50}$$

$$\emptyset_k = diag\left[e^{j\omega_o(T_k(\theta_1,\emptyset_1))}, \dots, e^{j\omega_o(T_k(\theta_p,\emptyset_p))}\right] \qquad k = y, z \tag{5.51}$$

$$A = [a_1 \dots a_p] \tag{5.52}$$

Where

$$a_i(\theta_i, \emptyset_i) = \left[e^{j\omega_o(\tau_1(\theta_i,\emptyset_i))}, \dots, e^{j\omega_o(T_N(\theta_i,\emptyset_i))}\right]^T \tag{5.53}$$

and

$$n_k = [n_{k,1}(t) \dots n_{k,N}(t)] \qquad k = x, y, z \tag{5.54}$$

The columns of A are assumed to be linearly independent. It is also assumed that the signal sub-space has dimension P [6]. Here

$$E[n_x(t)n_x(t)^H] = \sigma^2 I_N \tag{5.55}$$

$$E[n_x(t)n_y(t)^H] = \sigma^2 N_{xy} \tag{5.56}$$

$$E[n_x(t)n_z(t)^H] = \sigma^2 N_{xz} \tag{5.57}$$

Problem solution: We define the auto and cross covariance matrices as follow [6]

$$R_{xx} = E\{xx^H\} \tag{5.58}$$

$$R_{xy} = E\{xy^H\} \tag{5.59}$$

$$R_{xz} = E\{xz^H\} \tag{5.60}$$

We then have

$$R_{xx} = APA^H + \sigma^2 I_N \tag{5.61}$$

$$R_{xk} = AP\emptyset_k{}^H A^H + \sigma^2 N_{xk} \tag{5.62}$$

The noiseless auto and cross covariance matrices [6] are

32

$$C_{xx} = R_{xx} - \sigma^2 I_N = APA^H \tag{5.63}$$

$$C_{xk} = R_{xk} - \sigma^2 N_{xk} = AP\emptyset_k{}^H A^H \tag{5.64}$$

Solving for the eigen values of the matrix pencil (C_{xx}, C_{xk}), $k = y, z$ [6]

we obtain

$$|C_{xx} - \lambda_k C_{xk}| = 0 \tag{5.65}$$

$$\left|APA^H - \lambda_k AP\emptyset_k{}^H A^H\right| = 0 \tag{5.66}$$

$$AP|I - \lambda_k \emptyset_k|A^H = 0 \tag{5.67}$$

The eign values of the above matrix pencils $\lambda_{k,i}$, $1 \le i \le p$ give the diagonal values of $\emptyset_y$ for $k = z$ respectively. The problem now is to pair the right $\lambda_{y,i}$ to $\lambda_{z,j}$, $1 \le i, j \le p$, to obtain the correct pairing of DOAs [6].

Proposed Approach: We define the signal subspace E_s as the set of eigen vectors corresponding to generalized eigen values of the matrix pencil (C_{xx}, C_{xy}). Assumed that all the eigen values are arranged in the descending order [6].

We define a new marker matrix D as [30]

$$D = diag[r_1, r_2, \dots, r_p] \tag{5.68}$$

We now construct the mark auto and cross covariance matrices are [30]

$$C_{xxm} = E_s^H C_{xx} E_s D \tag{5.69}$$

$$C_{xkm} = E_s^H C_{xk} E_s \qquad k = y, z \tag{5.70}$$

Solving for the eign values of the matrix pencils (C_{xxm}, C_{xkm}), $k = y, z$, we get

$$|C_{xxm} - \lambda_k C_{xkm}| = 0 \tag{5.71}$$

$$\left|E_s^H C_{xx} E_s D - \lambda_k E_s^H C_{xk} E_s\right| = 0 \tag{5.72}$$

$$\left|E_s^H APA^H E_s D - \lambda_k E_s^H AP\emptyset_k{}^H A^H E_s\right| = 0 \tag{5.73}$$

To simplify the above equation we use the following two lemmas [6]

Lemma 1: Let $M = A^H E_s$ then M is a column permutation of a diagonal matrix [

Lemma 2: Consider matrix M a column permutation of a diagonal matrix and D a diagonal matrix. Then $MD = D_1 M$ where D_1 is the matrix D ,with its diagonal entries shuffled.

Using the above two lemmas

$$A^H E_s D = D_1 A^H E_s \tag{5.74}$$

Where D_1 is the D matrix with its diagonal entries shuffled. There for equation (5.73) becomes [6]

$$\left| E_s^H A P D_1 A^H E_s - \lambda_k E_s^H A P \emptyset_k^{\ H} A^H E_s \right| = 0 \tag{5.75}$$

$$E_s^H A P \left| D_1 - \lambda_k \emptyset_k^{\ H} \right| A^H E_s = 0 \tag{5.76}$$

From the structure of the equation (5.76) it is seen that

$$\lambda_{ym,i} = p_{1j} \gamma_{y,j} \qquad 1 \le i,j \le p \tag{5.77}$$

$$\lambda_{zm,i} = p_{1j} \gamma_{z,j} \qquad 1 \le i,j \le p \tag{5.78}$$

Where p_{1j} $1 \le j \le p$, is the jth diagonal entry of D_1. $\gamma_{y,j}$ and $\gamma_{z,j}$, $1 \le j \le p$ are the jth diagonal term of $\emptyset_y$ and $\emptyset_z$ respectively [6].

Hence we see that the correct eigenvalue pairs are multiplied by the same and unique entry from D_1.

The DOA of the sources can now be estimated from the following equations [6]

$$\theta_i = sin^{-1} \left[\frac{\propto_i}{u_y cos\emptyset - v_y sin\theta} \right] \qquad 1 \le i \le p \tag{5.79}$$

$$\emptyset_i = tan^{-1} \left[\frac{u_z \propto_i - u_y}{v_y - v_z \propto_i} \right] \qquad 1 \le i \le p \tag{5.80}$$

Where

$$\propto_i = \frac{log\gamma_{y,j}}{log\gamma_{z,j}} \qquad 1 \le i \le p$$

6

Results and discussion

In this chapter we compare and discuss the estimated DOA performance of MUSIC Algorithm with ESPRITS Algorithm. We also study the DOA estimated by using ESPRIT algorithm for planar array and then generate the beam in the same direction.

In the first part we compare the DOA estimated by using MUSIC and ESPRIT algorithm for linear array. In Figure 6.1 we use a MUSIC algorithm to estimate the angle of arrival, in this case we use fifteen sensors (no of antenna elements) and each two elements have a distance of 0.5λ. We use an angle of 30° and the resulted estimated angle is almost 30.98^o. By keeping the same no of elements and distance between the elements, we estimate the angles for $45^o, 60^o, 90^0$ $i.e.$ figure $6.2 - 6.4$. In figure 6.5 we double the no of sources for the same array as mentioned above, in this case we use an angles of 15° and 35°. It is observed in figure 6.5 that our estimated angles are almost 15.91^o and 35.87^o. In figure 6.6 we use three sources having an angles of $40^o, 60^o$ and 80° respectively, in this case again we kept the same distance between the elements, but we use 20 elements. The estimated angles are almost $40.88^o, 60.94^o$ and 80.76^o as shown in Figure 6.6. We observe in all cases that the difference between the original angles and estimated angles are almost 1° as shown in table 6.1.

Table 6.1 Estimation of DOA using ESPRIT Algorithm

No. of Elements	Distance	Angle	MUSIC Estimated Angle	ESPRIT Estimated Angle	MUSIC Difference	ESPRIT Difference
15	0.5	30	30.98	30.107	-0.98	-0.107
15	0.5	45	46	45.024	-1	-0.024
15	0.5	60	60.94	59.829	-0.94	0.171
15	0.5	90	91	89.300	-1	0.7

Mean= 0 and Variance = 0.1

We also estimate DOAs by using ESPRIT algorithm and results are shown in Table 6.1. It should be noted that in our case, the ESPRIT algorithm can estimate only one angle. From the it is shown in Table 6.1 that an array of fifteen elements are used, where each two elements have a distance 0.5λ. It is observed that the

estimated angles are 30.107°, 45.024°, 59.829° and 89.300° for the case of 30°, 45°, 59° and 90° respectively. The results shows that the difference between the original and estimated angles is small in case of ESPRIT algorithm as compared to MUSIC algorithm . Thus from these results one can conclude that ESPRIT algorithm is more accurate and better then MUSIC algorithm.

Table 6.2 Estimation of DOA using Planar Array

No. of Elements	Distance	Angles		Mean	Variance	Estimated Angle		Difference	
		θ	ϕ			θ	ϕ	θ	ϕ
5 x 5	0.5	30	60	0	0.1	29.998	59.989	0.002	0.011
5 x 5	0.5	60	60	0	0.1	59.997	59.997	0.003	0.003
5 x 5	0.5	45	45	0	0.1	44.989	45.005	0.011	-0.005
5 x 5	0.5	75	60	0	0.1	75.017	60.023	-0.017	-0.023
5 x 5	0.5	90	180	0	0.1	89.850	179.99	.150	0.01
10 x 10	0.5	30	60	0	0.1	29.989	60.078	0.011	-0.078
10 x 10	0.5	60	60	0	0.1	60.003	60.002	-0.003	-0.002
10 x 10	0.5	45	45	0	0.1	45.015	44.994	-0.015	0.006
10 x 10	0.5	75	60	0	0.1	74.991	60.001	0.009	-0.001
20 x 20	0.5	30	60	0	0.1	29.998	59.994	0.002	0.006
20 x 20	0.5	45	45	0	0.1	44.997	44.996	0.003	0.004
20 x 20	0.5	60	30	0	0.1	59.999	30.001	0.001	-0.001

Azimuth Angle(θ), Elevation Angle(ϕ)
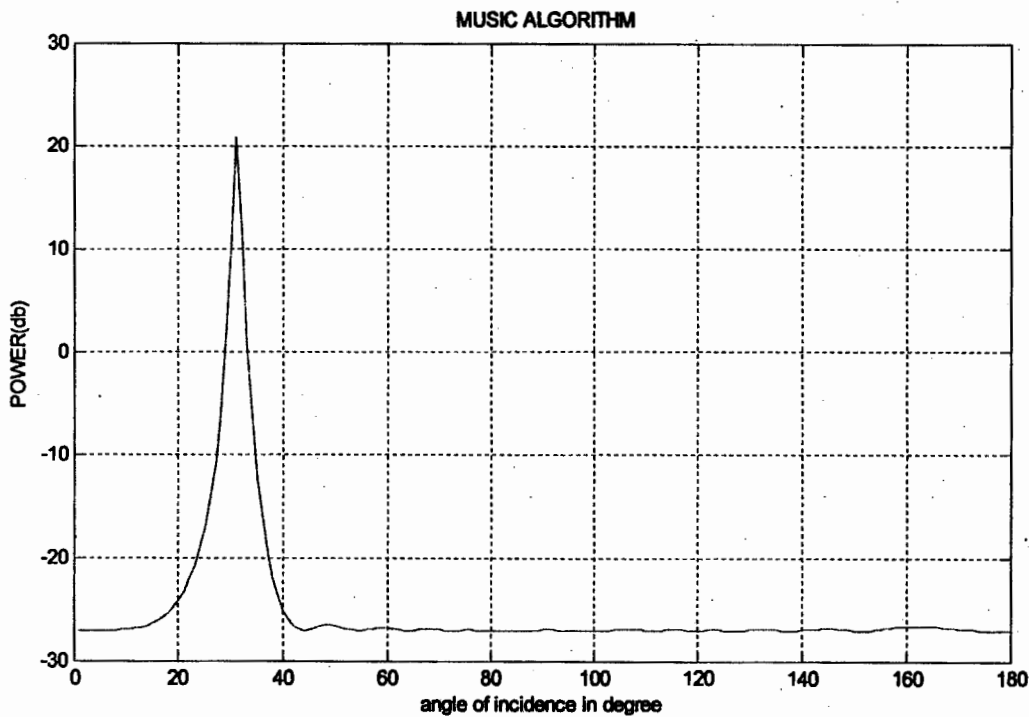

Figure 6.1 Estimation of DOA using MUSIC Algorithm for $\theta = 30°(N = 15, d_x = 0.5)$
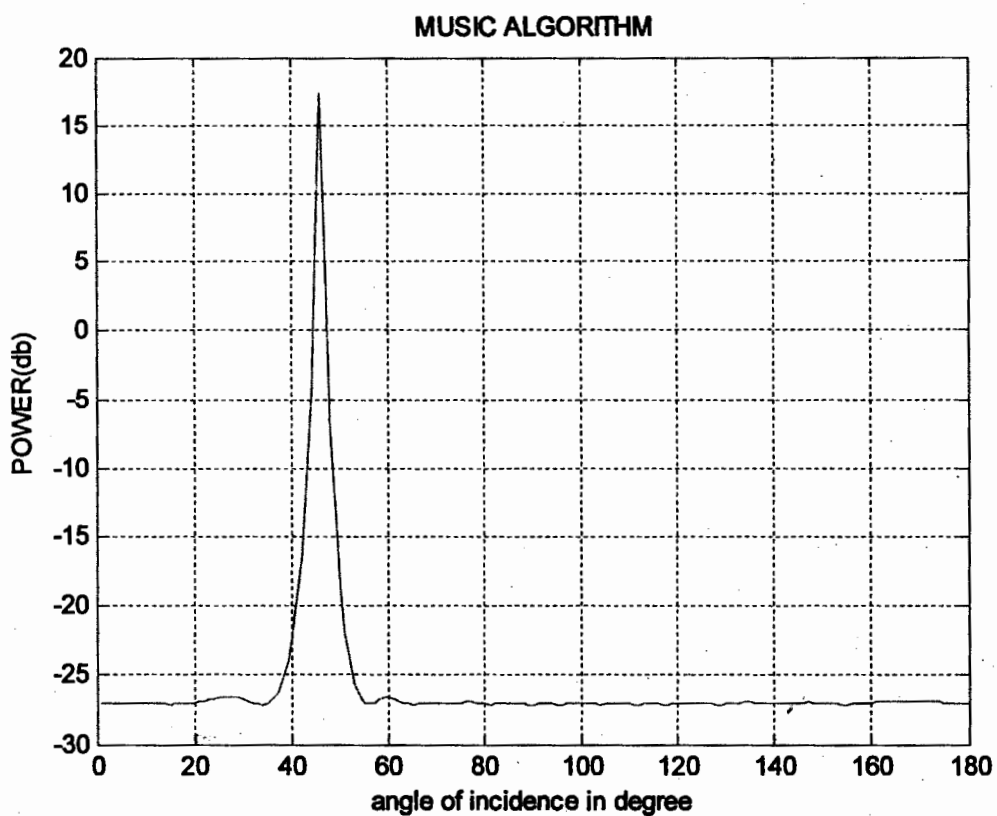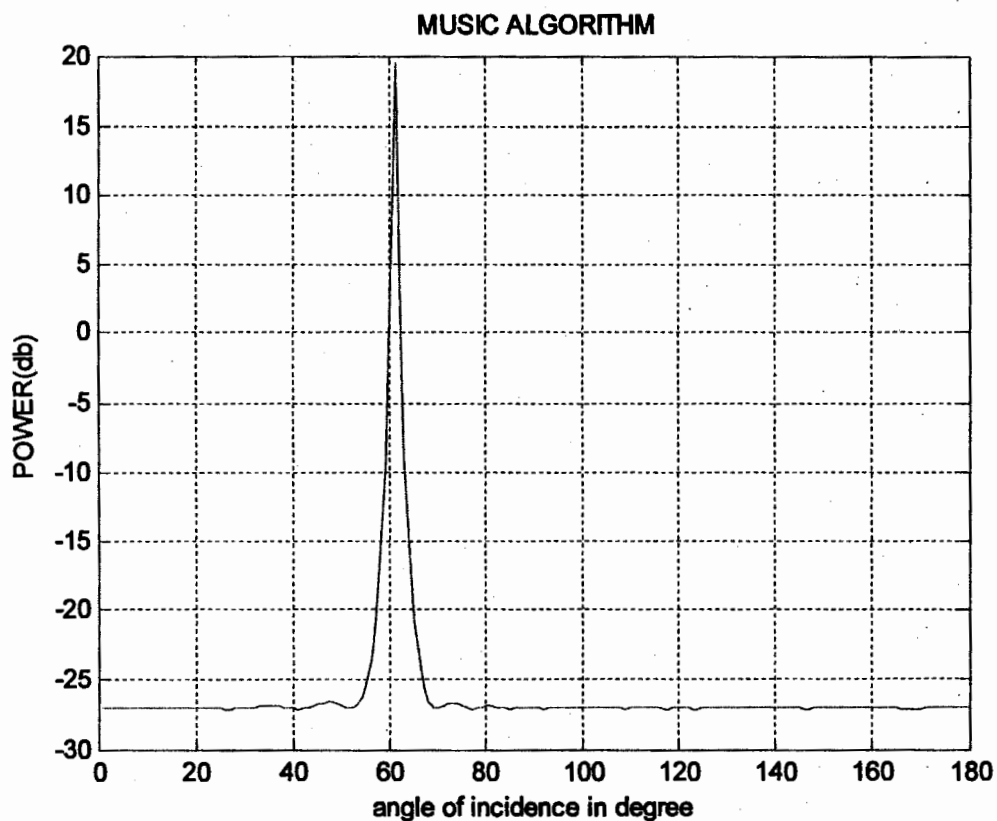
Figure 6.2 Estimation of DOA using MUSIC Algorithm for $\theta = 45^o (N = 15, d_x = 0.5)$

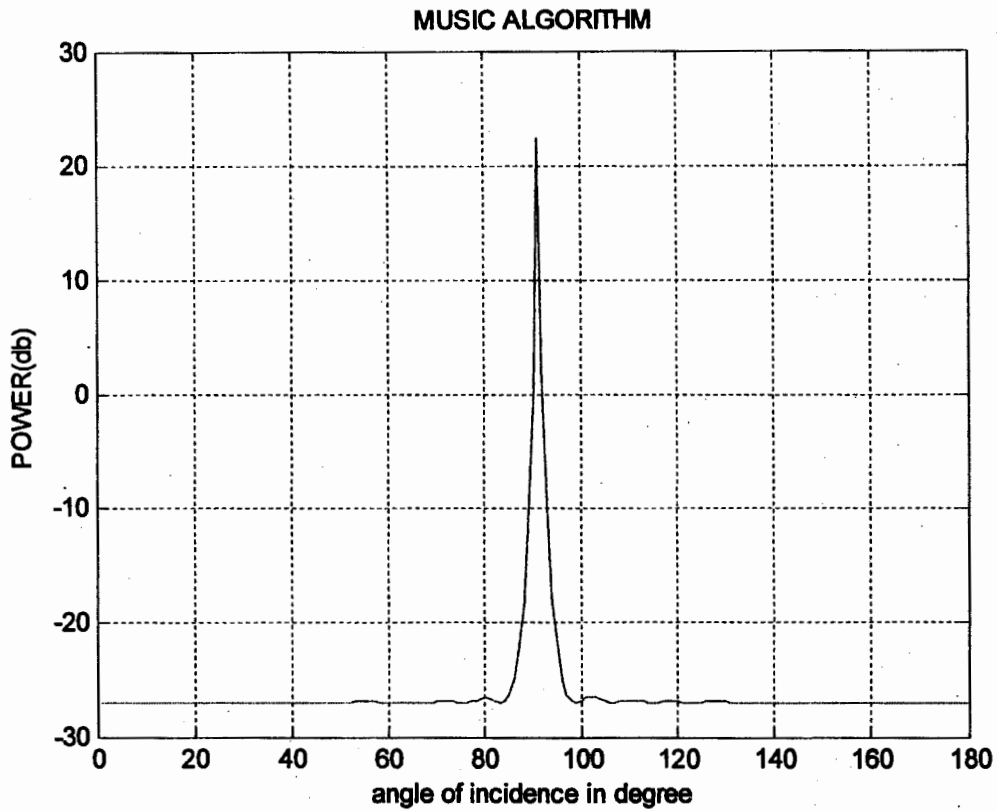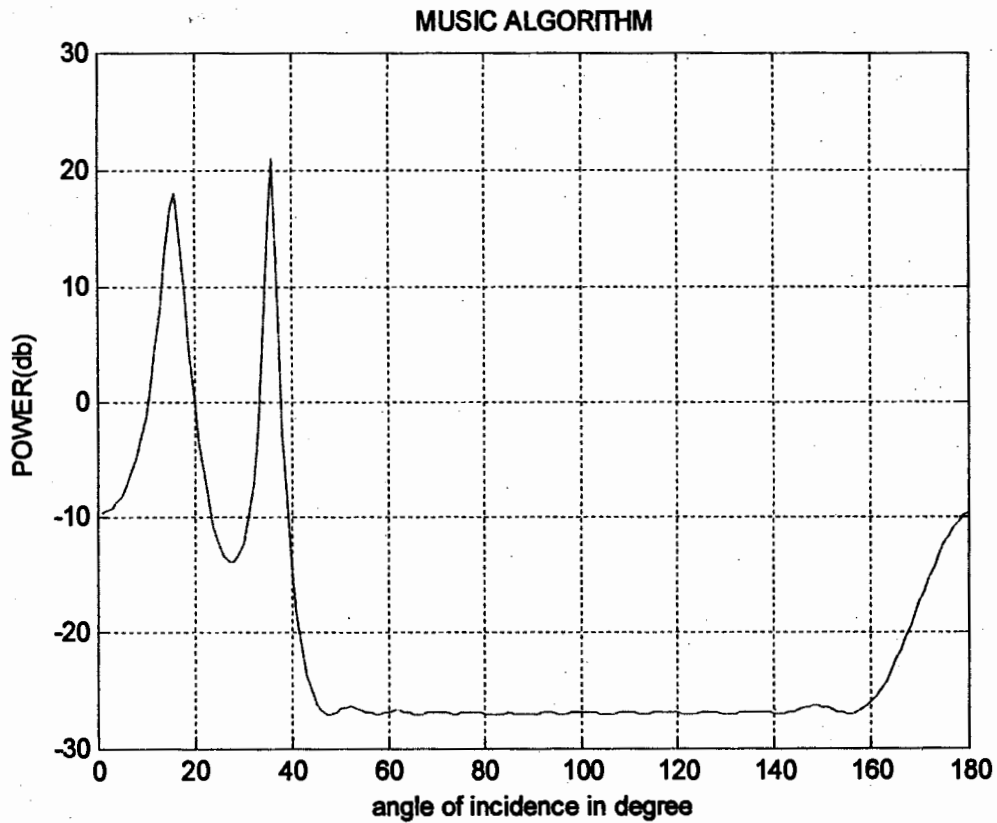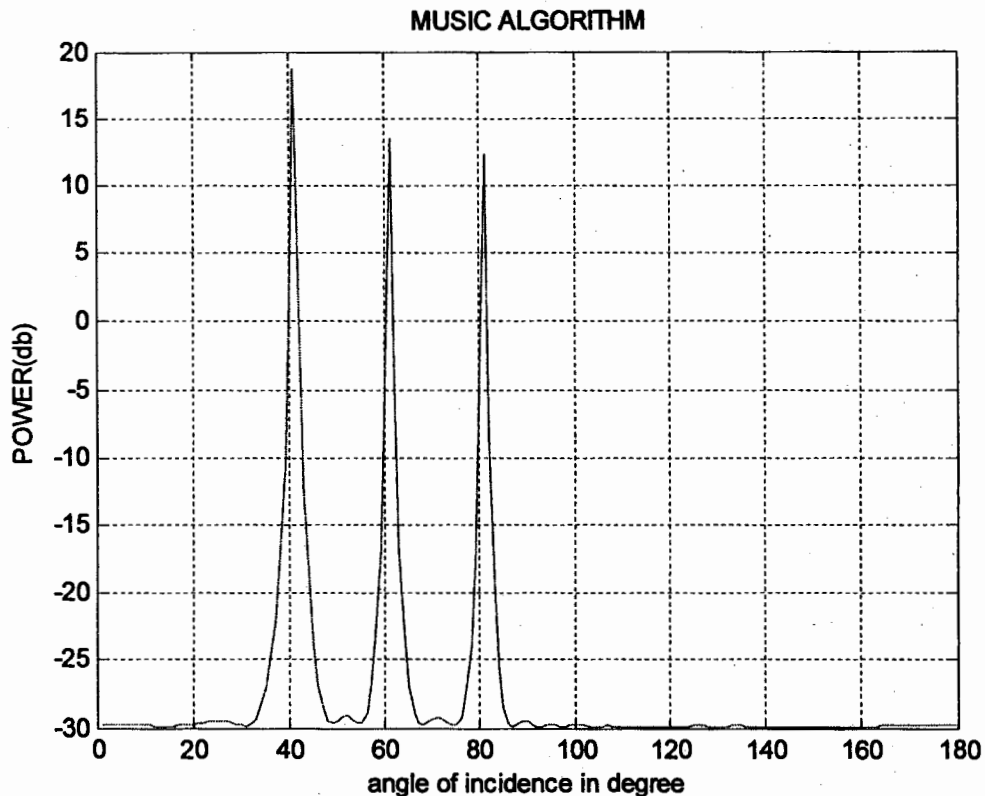Figure 6.3 Estimation of DOA using MUSIC Algorithm for $\theta = 60^o (N = 15, d_x = 0.5)$

MUSIC ALGORITHM

Figure 6.4 Estimation of DOA using MUSIC Algorithm for $\theta = 90^o (N = 15, d_x = 0.5)$

MUSIC ALGORITHM

Figure 6.5 Estimation of DOA using MUSIC Algorithm for $\theta = 15^o\ and\ 35^o (N = 15, d_x = 0.5)$

MUSIC ALGORITHM

Figure 6.6 Estimation of DOA using MUSIC Algorithm for $\theta = 40^o, 60^o \text{ and } 80^o (N = 20, d_x = 0.5)$

In our second part figure $6.7 - 6.20$ we use ESPRIT algorithm for planar array to estimate both azimuth (θ) and elevation angles ($\emptyset$). It should be noted again that in our case, it can estimate the DOA of a single source. In figure $6.7 - 6.10$ we use a planar array having five elements along $X - axis$ and five elements along $Y - axis$, the distance between the elements along $X - axis$ and along $Y - axis$ is $d_x = d_y = 0.5\lambda$. In our simulation, the value of mean and variance of a noise is equal to zero (0) and $(0 \cdot 1)$ respectively. The azimuth and elevation angles estimate are $(29.998^o, 59.989^o)$, $(44.989^o, 45.005^o)$,$(75.017^o, 60.023^o)$ and $(79.850^o, 179.99)^o$ respectively for the case of $(30^o, 60^o)$, $(60^o, 60^o)$, $(45^o, 45^o)$, $(75^o, 60^o)$ and $(90^o, 180^o)$ as shown in Table 6.2

Similarly we estimate DOAs for planar arrays having ten elements along $x - axis$ and ten elements along $y - axis$ as shown in Figure ($6.11 - 6.14$). The difference between the estimated and original angles are shown in table 6.2. In figure $6.15 - 6.17$ we use twenty elements along $x - axis$ and $y - axis$.

Figure 6.18 represents result for fifty iterations for the planar array having five elements along $x - axis$ and five elements along $y - axis$. From Figure 6.18 it is clear that all the spots which shows estimated angles are closer to $(30^o, 60^o)$. Similar results are shown for ten elements along $x - axis$ and ten elements along $y - axis$

in figure 6.19 . Figure 6.20 is sketch for the same specification as we discussed in figure 6.18 and figure 6.19 except that the number of elements along $x-axis$ and $y-axis$ are twenty.

In Figure $6.21-6.26$ we form the beam on the same estimated DOAs produced by the planar array. For example the planar array of Figure 6.7 first calculated the DOA by using ESPRIT algorithm and then generate the beam in the same direction as shown in Figure 6.21. Similar beams are shown in Figure $6.23-6.24$ and $6.25-6.26$ for the case of ten elements and twenty elements respectively. From figure $6.21-6.26$ it is clear that as we increase the number of elements of planar array ,the beams become more narrower and the directivity of planar array improves.
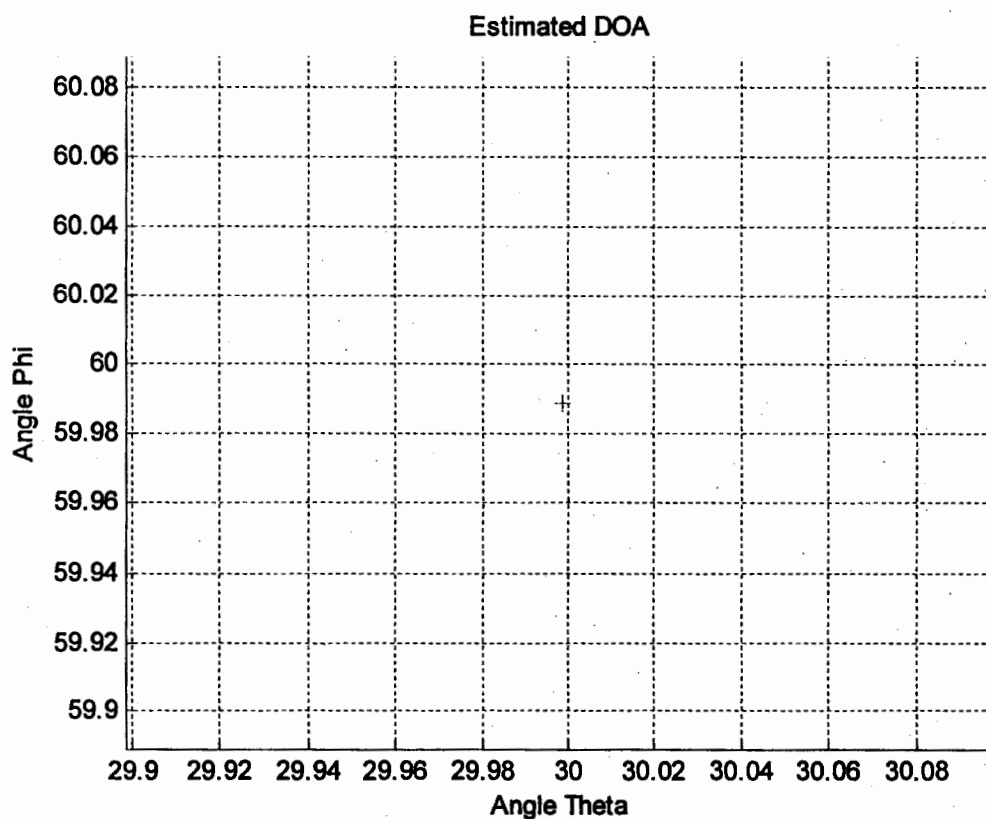
Figure 6.7 Estimation of DOA using ESPRIT Algorithm for $\theta = 30^o, \phi = 60^o$
$$\left(N = 5, M = 5, d_x = 0.5, d_y = 0.5, \text{ Mean} = 0, \text{ Var} = 0.1\right)$$

Estimated DOA

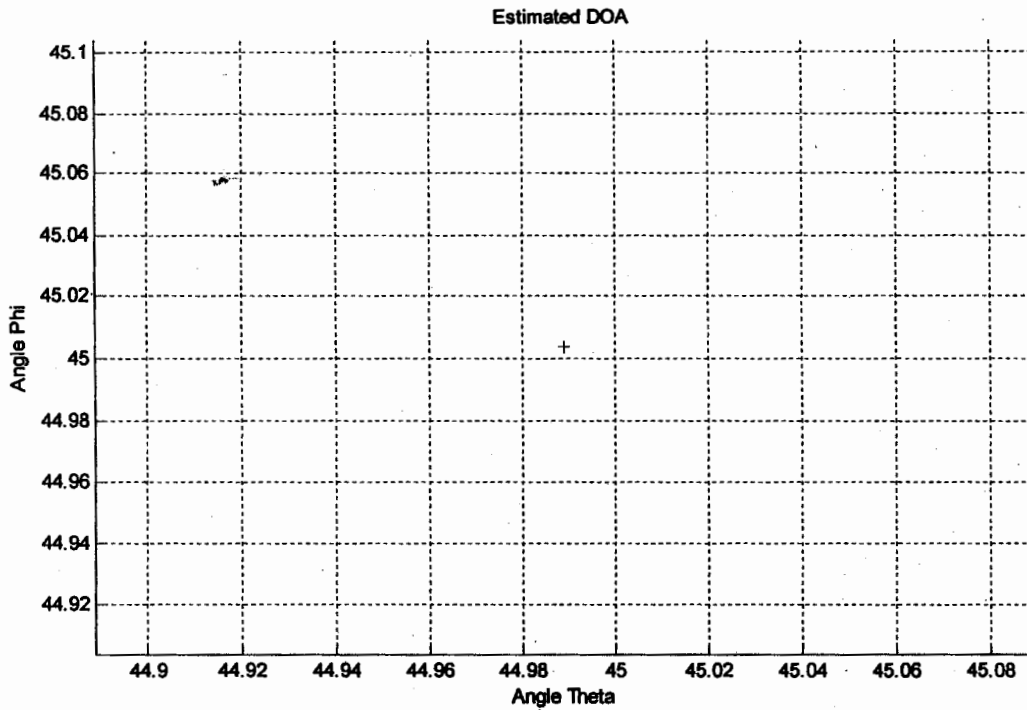Figure 6.8 Estimation of DOA using ESPRIT Algorithm for $\theta = 45^o, \phi = 45^o$
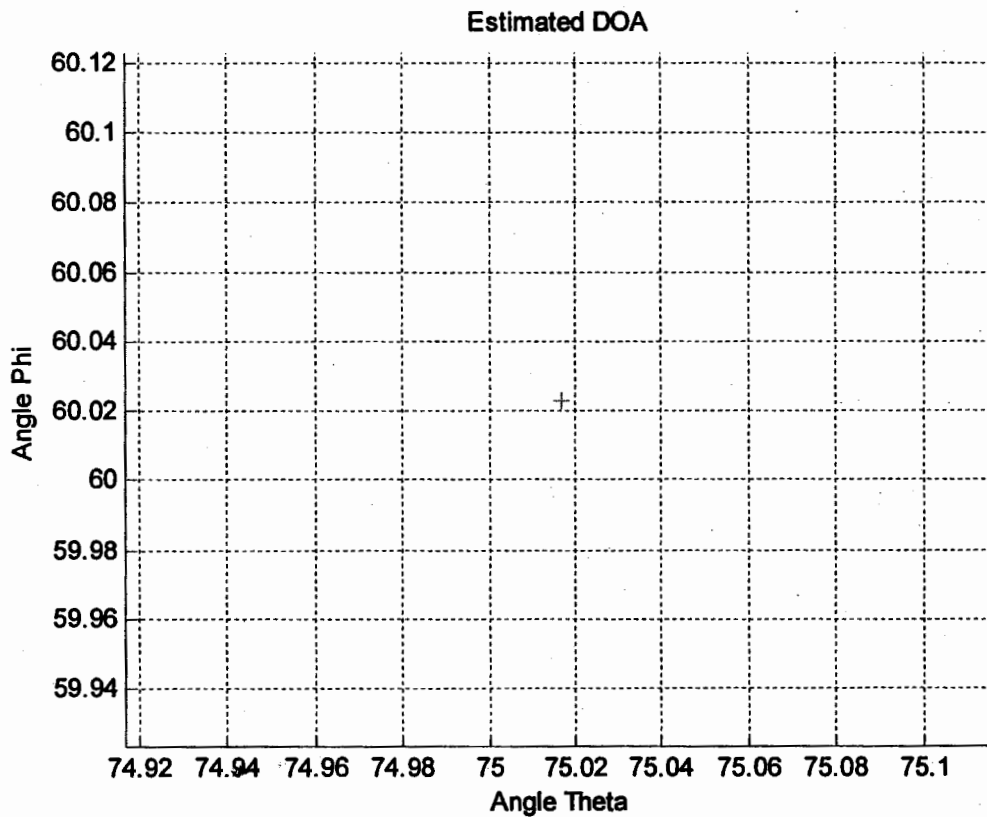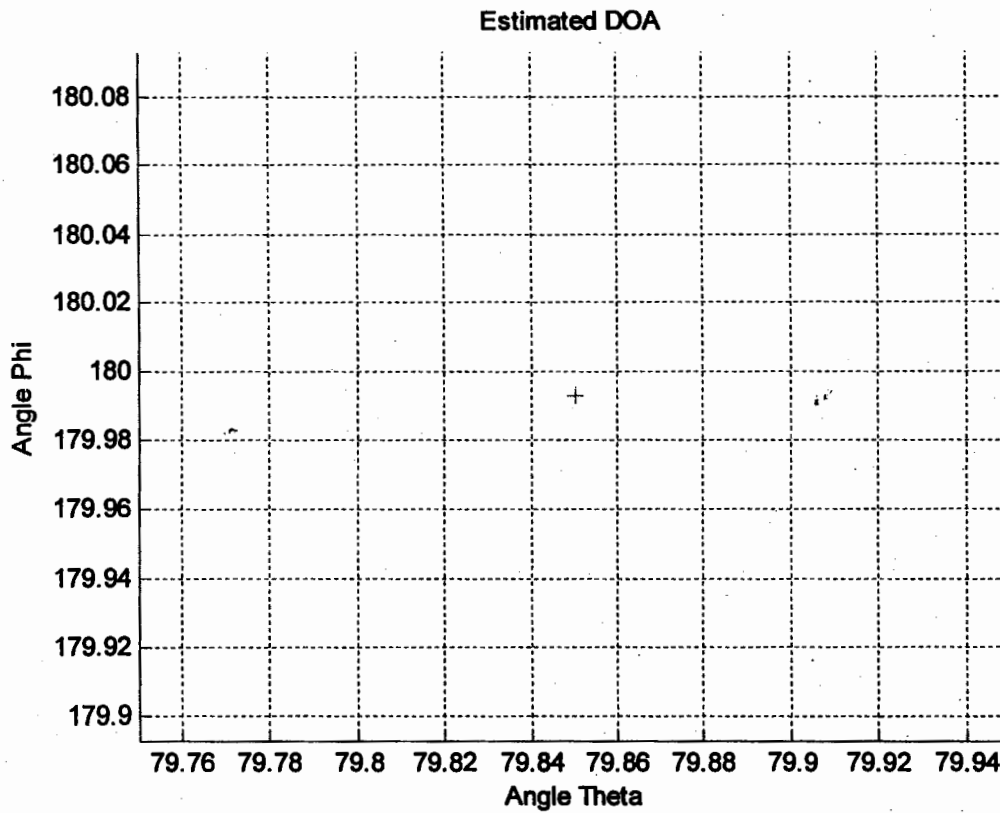$\left(N = 5, M = 5, d_x = 0.5, d_y = 0.5, \text{ Mean} = 0, \text{ Var} = 0.1\right)$

Estimated DOA

Figure 6.9 Estimation of DOA using ESPRIT Algorithm for $\theta = 75^o, \phi = 60^o$
$\left(N = 5, M = 5, d_x = 0.5, d_y = 0.5, \text{Mean} = 0, \text{ Var} = 0.1\right)$

Figure 6.10 Estimation of DOA using ESPRIT Algorithm for $\theta = 90^o, \phi = 180^o$
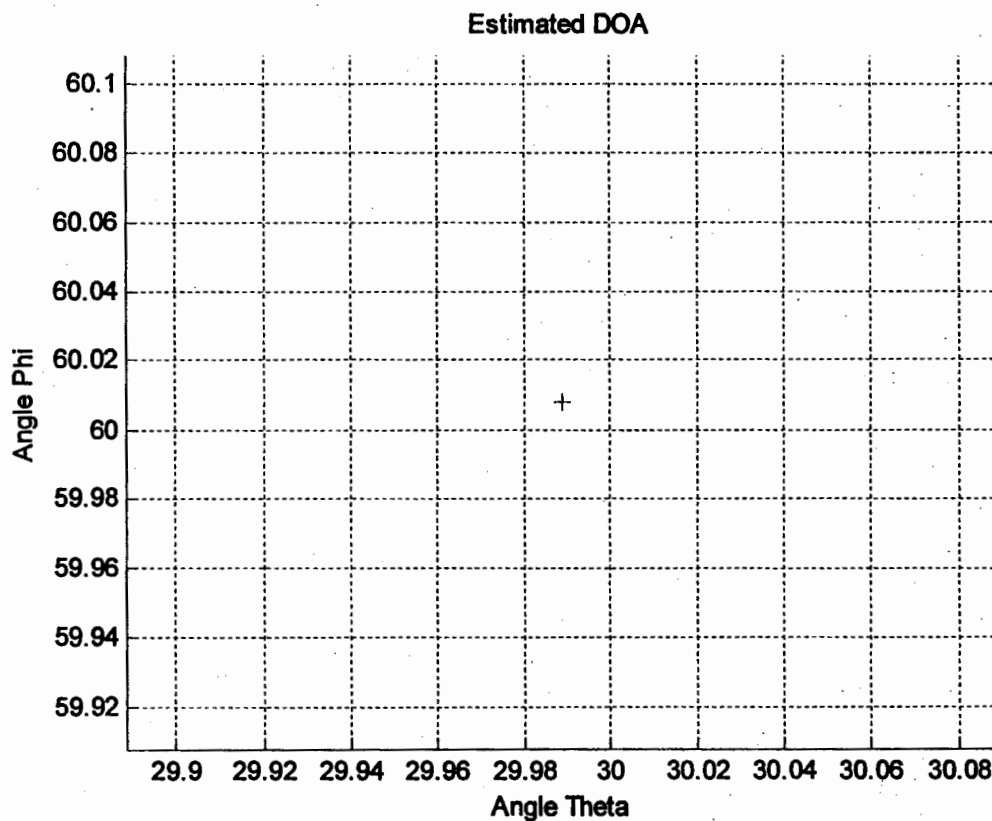$\left(N = 5, M = 5, d_x = 0.5, d_y = 0.5, \text{Mean} = 0, \text{Var} = 0.1\right)$

Figure 6.11 Estimation of DOA using ESPRIT Algorithm for $\theta = 30^o, \phi = 60^o$
$\left(N = 10, M = 10, d_x = 0.5, d_y = 0.5, \text{Mean} = 0, \text{Var} = 0.1\right)$
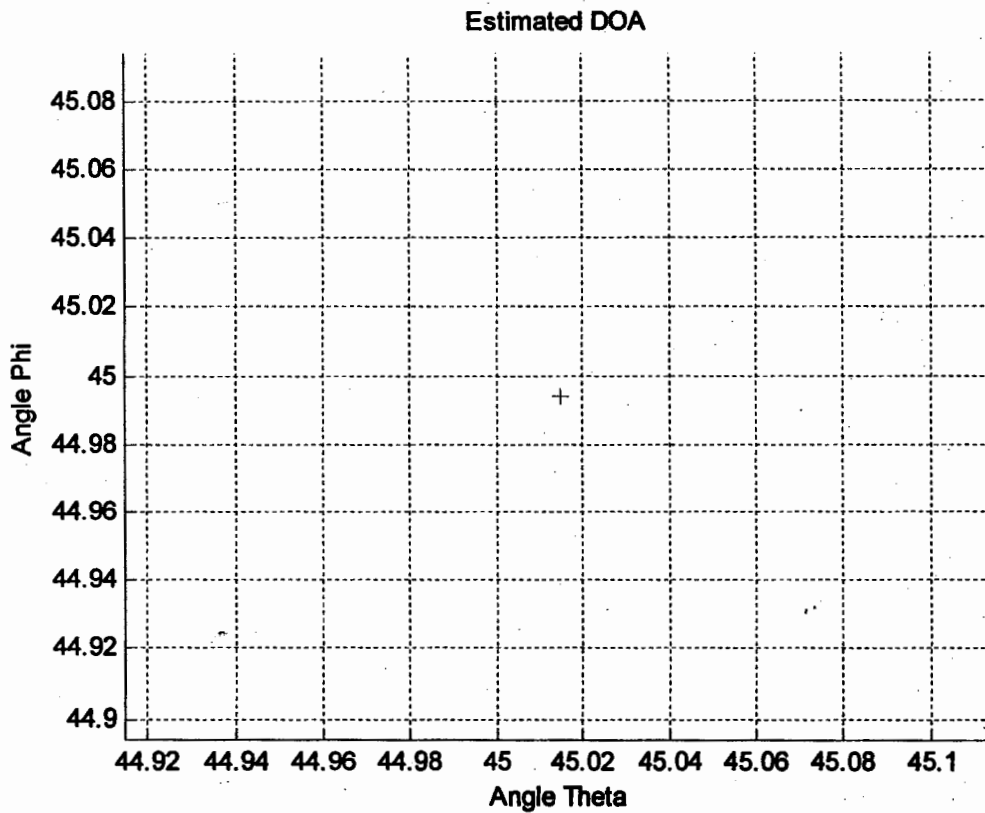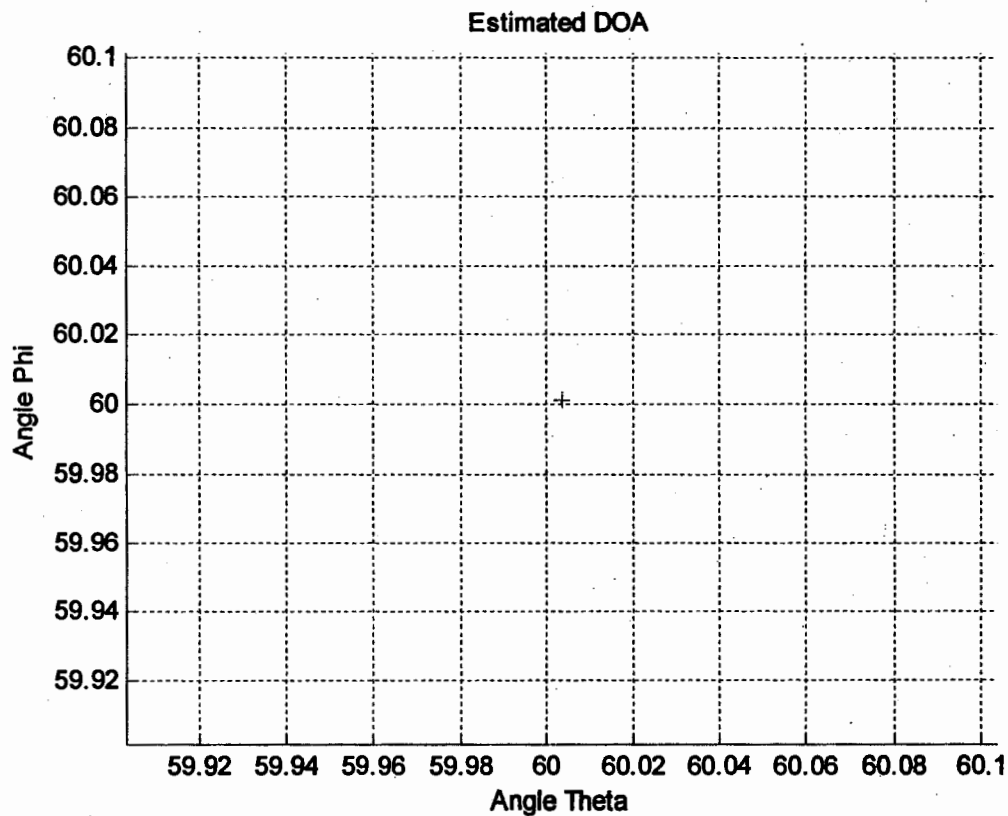
Figure 6.12 Estimation of DOA using ESPRIT Algorithm for $\theta = 45^o, \phi = 45^o$
$\left(N = 10, M = 10, d_x = 0.5, d_y = 0.5, \text{ Mean} = 0, \text{ Var} = 0.1\right)$

Figure 6.13 Estimation of DOA using ESPRIT Algorithm for $\theta = 60^o, \phi = 60^o$
$\left(N = 10, M = 10, d_x = 0.5, d_y = 0.5, \text{ Mean} = 0, \text{ Var} = 0.1\right)$
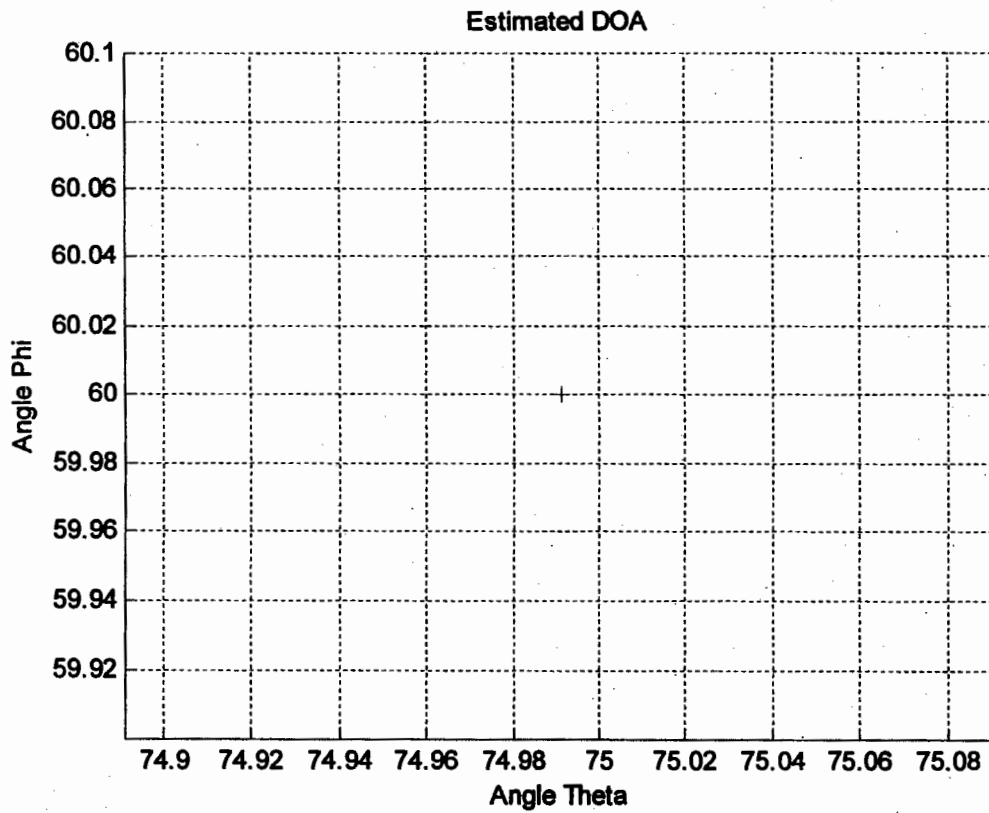
Estimated DOA

Figure 6.14 Estimation of DOA using ESPRIT Algorithm for $\theta = 75^o, \phi = 60^o$
$\left(N = 10, M = 10, d_x = 0.5, d_y = 0.5, \text{Mean} = 0, \text{ Var} = 0.1 \right)$
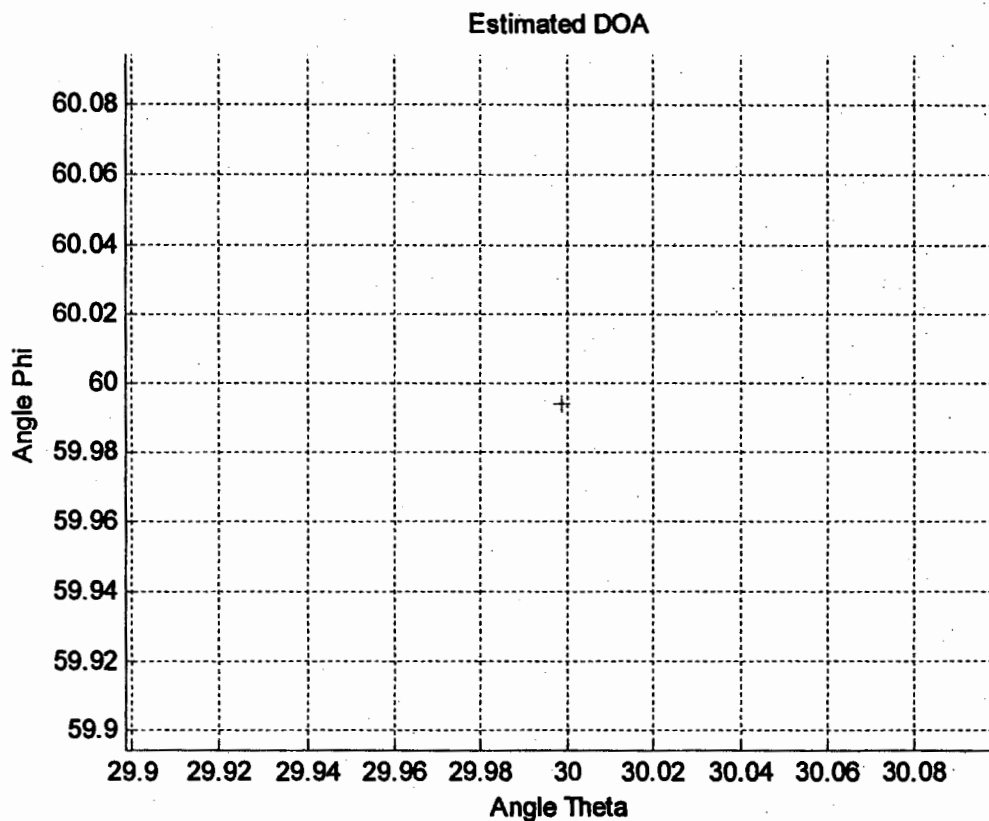
Estimated DOA

Figure 6.15 Estimation of DOA using ESPRIT Algorithm for $\theta = 30^o, \phi = 60^o$
$\left(N = 20, M = 20, d_x = 0.5, d_y = 0.5, \text{Mean} = 0, \text{ Var} = 0.1 \right)$

Estimated DOA

Figure 6.16 Estimation of DOA using ESPRIT Algorithm for $\theta = 45^o, \phi = 45^o$
$\left(N = 20, M = 20, d_x = 0.5, d_y = 0.5, \text{ Mean} = 0, \text{ Var} = 0.1\right)$

Estimated DOA

Figure 6.17 Estimation of DOA using ESPRIT Algorithm for $\theta = 60^o, \phi = 30^o$
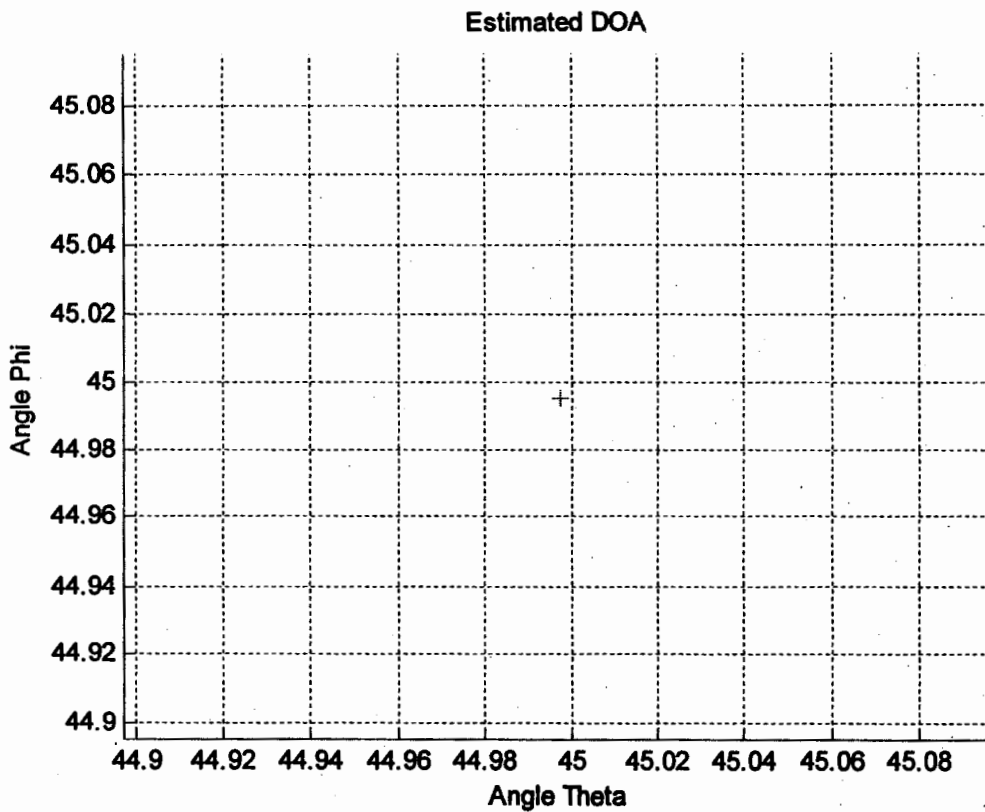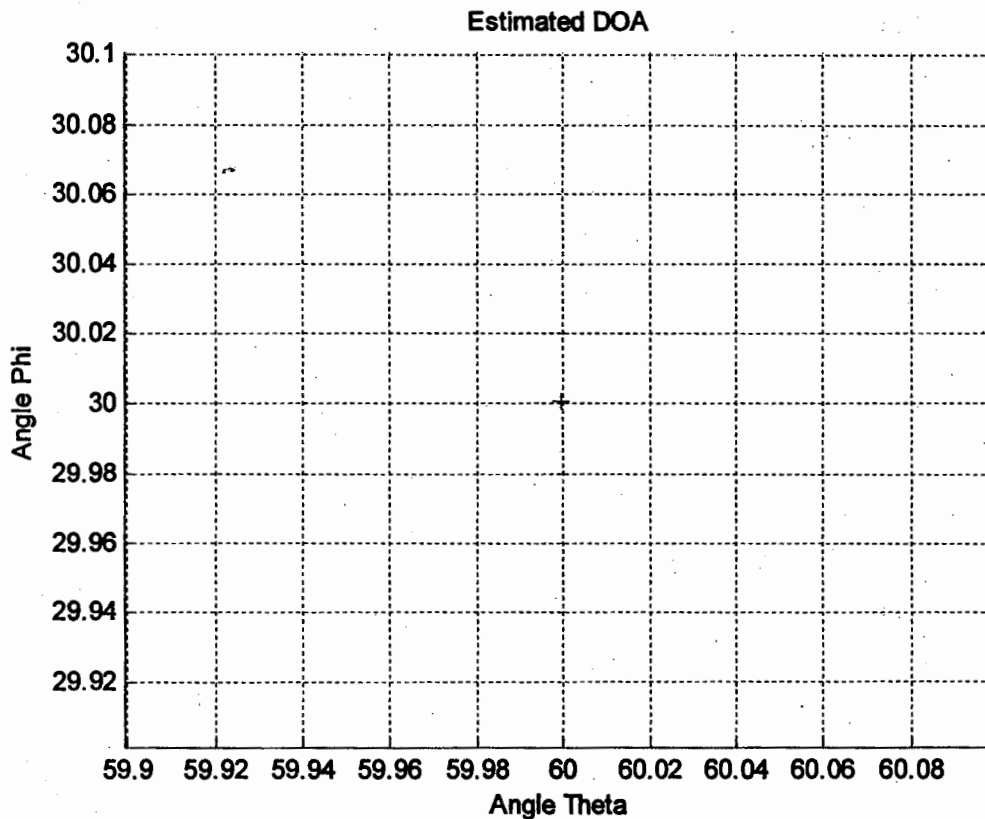$\left(N = 20, M = 20, d_x = 0.5, d_y = 0.5, \text{ Mean} = 0, \text{ Var} = 0.1\right)$

Figure 6.18 Estimation of DOA using ESPRIT Algorithm for no. of iterations= 50,
$(\theta = 30^o, \phi = 60^o)$ $(N = 5, M = 5, d_x = 0.5, d_y = 0.5, \text{Mean} = 0, \text{Var} = 0.1)$

Figure 6.19 Estimation of DOA using ESPRIT Algorithm for no. of iterations= 50,
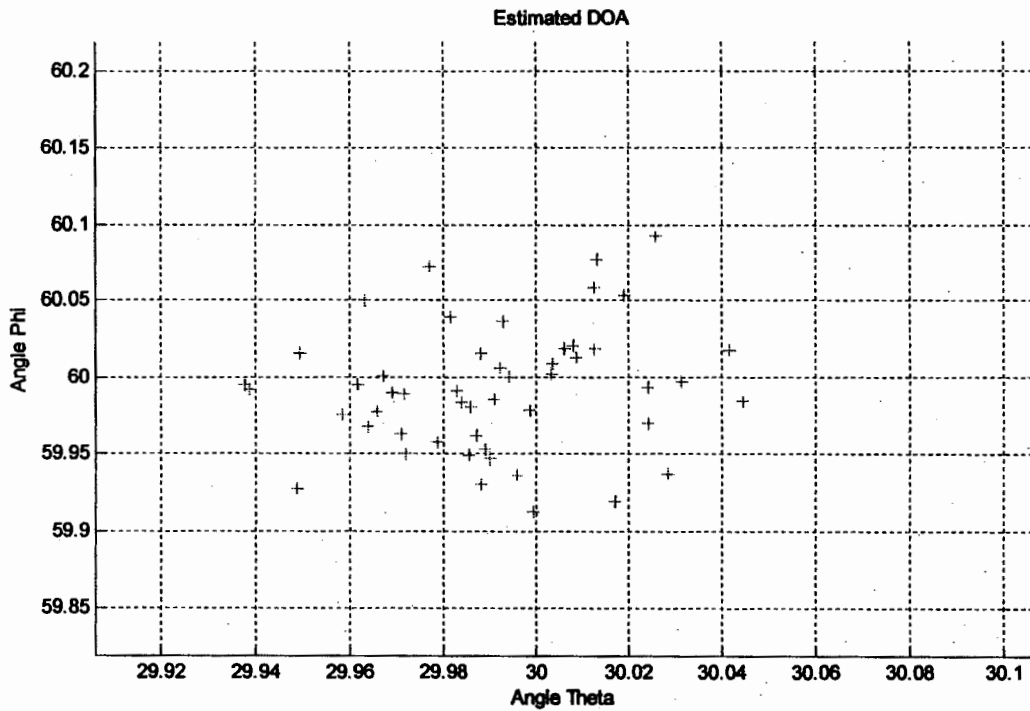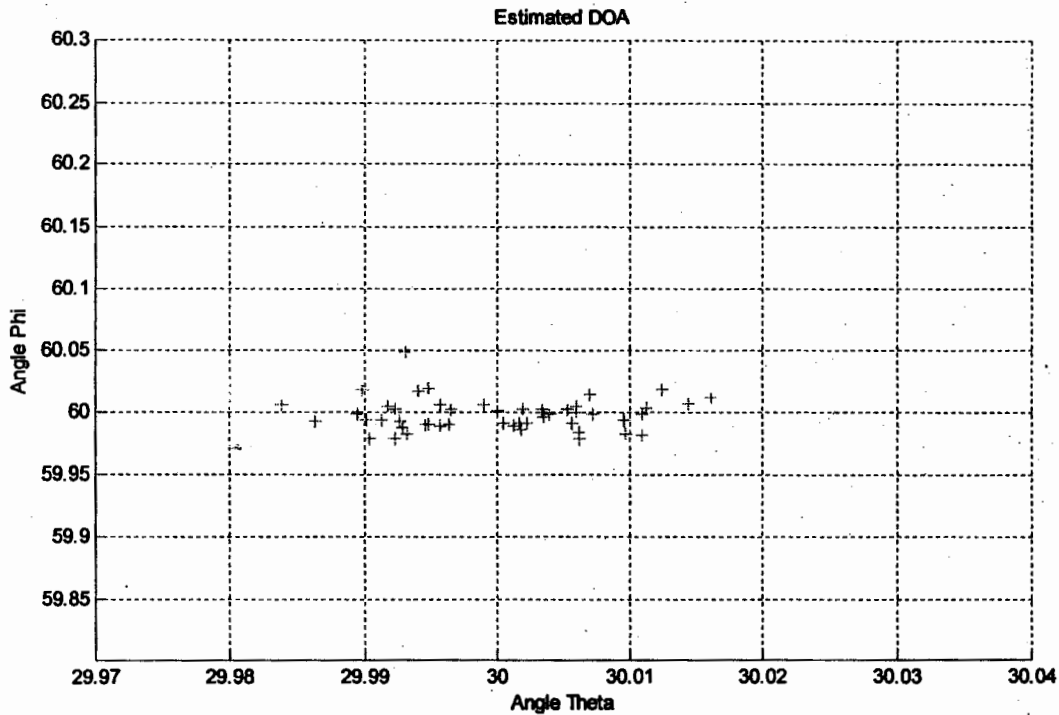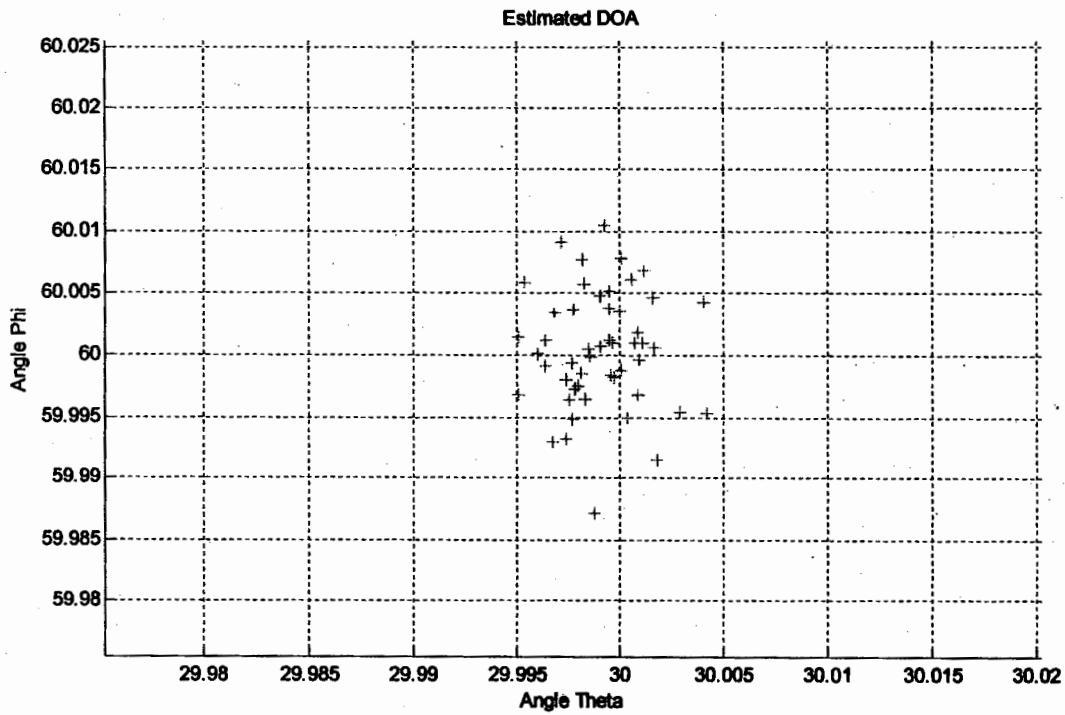$(\theta = 30^o, \phi = 60^o)$ $(N = 10, M = 10, d_x = 0.5, d_y = 0.5, \text{Mean} = 0, \text{Var} = 0.1)$

Figure 6.20 Estimation of DOA using ESPRIT Algorithm for no. of iterations= 50,
$(\theta = 30^o, \phi = 60^o)$ $(N = 20, M = 20, d_x = 0.5, d_y = 0.5, \text{Mean} = 0,\ \text{Var} = 0.1)$

Figure 6.21 Beamforming at estimated DOA $(\theta = 30^o, \phi = 60^o)$ using Planar Array
for $(N = 5, M = 5, d_x = 0.5, d_y = 0.5)$

Figure 6.22 Beamforming at estimated DOA $(\theta = 45^o, \phi = 45^o)$ using Planar Array for $(N = 5, M = 5, d_x = 0.5, d_y = 0.5)$
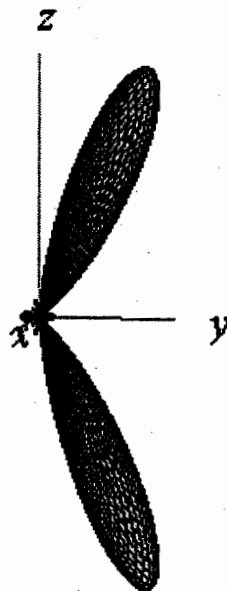

Figure 6.23 Beamforming at estimated DOA $(\theta = 30^o, \phi = 60^o)$ using Planar Array for $(N = 10, M = 10, d_x = 0.5, d_y = 0.5)$

Figure 6.24 Beamforming at estimated DOA ($\theta = 45°, \phi = 45°$) using Planar Array for $\left(N = 10, M = 10, d_x = 0.5, d_v = 0.5\right)$

Figure 6.25 Beamforming at estimated DOA ($\theta = 30°, \phi = 60°$) using Planar Array for $\left(N = 20, M = 20, d_x = 0.5, d_y = 0.5\right)$

Figure 6.26 Beamforming at estimated DOA $(\theta = 45^o, \phi = 45^o)$ using Planar Array for $\left(N = 20, M = 20, d_x = 0.5, d_y = 0.5\right)$
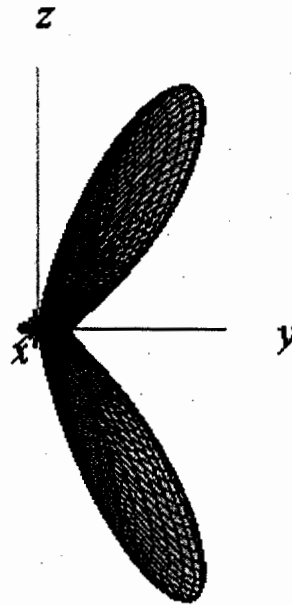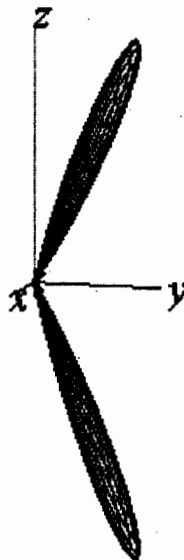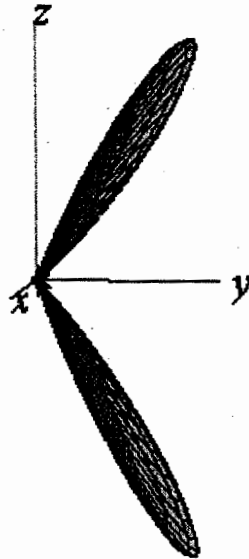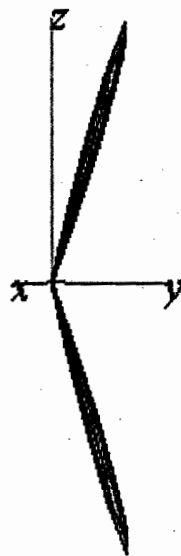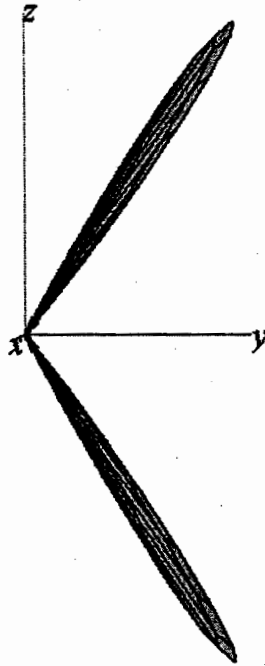
7

Conclusion and future work

7.1 Conclusion

In this work, we assume that a planar array is acting as radar. Whenever target is detected then our planar array is able to estimate angle of arrival accurately by using ESPRIT algorithm and at the same time it has been able to generate a beam in the same direction. We divided our work in two parts.

In the first part we estimated the DOA for linear array by using MUSIC and ESPRIT Algorithms. Then by taking different values of DOAs, we compared the estimated DOAs obtained from MUSIC and ESPRIT Algorithms. The results shows that ESPRIT algorithm is more accurate than MUSIC algorithm.

In the second part, we estimated the DOA (θ, ϕ) by using ESPRIT algorithm by using planar array and we also generate a beam on the estimated DOA (θ, ϕ). It is also shown that the directivity of a planar array improves with the increase in the number of elements.

7.2 Future Work

Future work of this study could involve an extension of the ESPRIT algorithm for more then one source . Also the algorithm can be tested in different signals propagation environments. Nulls can be generated adaptively for the interfering signals. Moreover the generated beam can be scanned anywhere in space.

Important Definitions

❖ **Antenna**

An antenna is defined by Webster's Dictionary as "a usually metallic device (as a rodor wire) for radiating or receiving radio waves." The IEEE Standard Definitions of Terms for Antennas (IEEE Std 145–1983) defines the antenna or aerial as "a means for radiating or receiving radio waves."

❖ **Major lobe**

A major lobe (also called main beam) is defined as "the radiation lobe containing the direction of maximum radiation."

❖ **Minor lobe**

A minor lobe is any lobe except a major lobe. Minor lobes usually represent radiation in undesired directions.

❖ **Side lobe**

A side lobe is "a radiation lobe in any direction then than the intended lobe." (Usually a side lobe is adjacent to the main lobe and occupies the hemisphere in the direction of the main beam.). Side lobes are normally the largest of the minor lobes.

❖ **Back lobe**

A back lobe is "a radiation lobe whose axis makes an angle of approximately 180° with respect to the beam of an antenna." Usually it refers to a minor lobe that occupies the hemisphere in a direction opposite to that of the major (main) lobe.

❖ **Coherence Bandwidth**

Coherence bandwidth is the statistical measure of the range of frequencies over which the channel can be considered flat. In other words in this bandwidth the channel passes all spectral components with approximately equal gain and linear phase.

These ranges of frequencies have a strong potential for amplitude correlation.

❖ **Coherence Time**

Coherence time is the statistical measure of the time duration over which the channel impulse response is essentially invariant and quantifies the similarity of the channel response at different time. In other words we can say that it is

the time duration over which two received signal have a strong potential for amplitude correlation.

❖ Antenna Gain

Gain of an antenna (in a given direction) is defined as "the ratio of the intensity, in a given direction, to the radiation intensity that would be obtained if the power accepted by the antenna were radiated isotropically. The radiation intensity corresponding to the isotropically radiated power is equal to the power accepted (input) by the antenna divided by 4π."

❖ Antenna Bandwidth

The bandwidth of an antenna is defined as "the range of frequencies within which the performance of the antenna, with respect to some characteristic, conforms to a specified standard." The bandwidth can be considered to be the range of frequencies, on either side of a center frequency, where the antenna characteristics (such as input impedance, pattern, beamwidth, polarization, side lobe level, gain, beam direction, radiation efficiency) are within an acceptable value of those at the center frequency.

Bibliography

[1] C. A. Balanis, *Antenna Theory: Analysis and design* CRC Press LLC, 2004.

[2] A. Paulraj, R. Roy and T. Kailath, "A subspace rotation approach to signal parameter estimation," *Proc. IEEE,* vol. 74, pp. 1044–1045, Jul. 1986.

[3] R. O. Schmidt, "Multiple emitter location and signal parameter estimation", *IEEE Trans. Antennas and Propagation* AP-34 (3) 278–279, 1986.

[4] R. Roy and T. Kailath, "ESPRIT—estimation of signal parameters via rotational invariance techniques" *IEEE Trans. Acoust., Speech, Signal Process.,* vol. 37, no. 7, pp. 984–995, Jul. 1989.

[5] T.H. Liu, J.M. Mendel, "Azimuth and elevation direction 0ndingusing arbitrary array geometries," *IEEE Trans. Signal Process.* Vol. 46 (7) pp. 2061–2065, 1998.

[6] V.S. Kedia, B. Chandna, "A new algorithm for 2-D DOA estimation," *Signal Process.* Vol. 60 pp. 325–332 1997.

[7] M.D. Zoltowski, M. Haardt, C.P. Mathews, "Closed-form 2-Dangle estimation with rectangular arrays in element space or beamspace via unitary ESPRIT," *IEEE Trans. Signal Process.* Vol. 44 (2) pp.316–328 1996.

[8] J. A Cadzow, "A high resolution direction of arrival algorithm for narrowband coherent and incoherent sources", *IEEE Trans. Acoust. Speech Signal Process.,* Vol. 3 , pp. 965-979, 1988.

[9] R. H. Roy, "ESPRIT-Estimation of signal parameters via rotational invariance techniques." *Ph.D. dissertation, Stanford Univ. Stanford, CA,* 1987.

[10]   P. M. Shankar, *Introduction to Wireless Systems,* John Wiley & Sons, 2002.

[11]   Shinya Sekizawa, "Estimation of Arrival Directions Using MUSIC Algorithm with a Planar Array," *YRP Mobile Telecommunications Key Technology Research Laboratories Co., Ltd. 3-4 Hikari-no-oka, Yokosuka.*

[12]   S. Sekizawa, "Development of Liner Array Antenna System for Estimation of Arrival Angles of Multipath," *IEICE Technical Report, RCS 96-128,* pp. 7-14, Jan. 1997.

[13]   L. C. Godara, *Smart antennas* CRC Press LLC, 2004.

[14]   G. V. Tsoulos, "Smart antennas for mobile communication systems; benefits and challenges," *IEEE Commun. Eng. J.,* vol. 11, no. 2, pp. 84–94, Apr. 1999.

[15]   Y. T. Lo and S. W. Lee (Eds), *Antenna Handbook, Theory, Applications, and Design,* Van Nostrand Reinhold Company, New York, 1988.

[16]   J. C. Liberti and T. S. Rappaport, *Smart Antennas for Wireless Communications*: IS-95 and Third Generation CDMA Applications. Upper Saddle River, NJ: Prentice Hall PTR, 1999.

[17]   Johnson, D., "The Application of Spectral Estimation Methods to Bearing Estimation Problems," *Proceedings of the IEEE,* Vol. 70, No. 9, pp. 1018–1028, Sept. 1982.

[18]   S. Haykin, *Adaptive Filter Theory,* Prentice Hall PTR, Upper Saddle River, NJ, 1996.

[19]   Shan, T-J., M. Wax, and T. Kailath, "Spatial Smoothing for Direction-of-Arrival Estimation of Coherent Signals," *IEEE Transactions on Acoustics, Speech, and Signal Processing,* Vol. ASSP-33, No. 4, pp. 806–811, Aug. 1985.

[20]   F. B. Gross, *Smart Antennas for Wireless Communications,* Prentice Hall, New York, 1999.

[21]   Godara, L., "Application of Antenna Arrays to Mobile Communications, Part II: Beam forming and Direction-of-Arrival Considerations," *Proceedings of the IEEE,* Vol. 85, No. 8, pp. 1195–1245, Aug. 1997.

[22]   I. Ziskind and M. Wax, "Maximum Likelihood Localization of Multiple Sources by Alternating Projection," *IEEE Trans. Acoustics, Speech, and Signal Process.,* Vol. 36, No. 10, pp. 1553–1560, Oct. 1988.

[23]   G. Xu and H. Liu, "An Effective Transmission Beamforming Scheme for Frequency-Division- Duplex Digital Wireless Communication Systems," *1995 International Conference on Acoustics, Speech, and Signal Processing,* Vol. 3, pp. 1729–1732, 1995.

[24]   B. J. Forman, "Beamwidth and directivity of large scanning array," *Radio Science,* Vol. 5 No. 7 , July 1970, pp. 1077-1083

[25]   John D. Kraus, *Antennas,* Mc Graw Hill, Singapore, 1998.

[26]   Abraham. M and R. Becker, *Electricity and Magnetism,* Stechert, 1932.

[27]   J. S. Stone, United States Patents *No. 1643323 and No. 1715433*

[28]   P. M. Shankar, *Introduction to Wireless Systems*, John Wiley & Sons, New York, 2002.

[29]   J. D. Kraus, *Radio Astronomy*, McGraw-Hill Book Co., 1966.

[30]   Chen, Y H, Chen C H. "Direction of Arrival and Frequency Estimation for Narrowband Sources Using Two Single Rotation Invariance Algorithms with the Marked Subspace," *IEE-F Proc. on Radar and Signal Proc.,* pp. 297-301, 1992.

[31]   T. S. Rappaprt, *Wireless Communication: Principle and Practice*, Prentice Hall, 1996.

Vita

The author was born in 1983 at Bannu He belongs to village Sikna Koat Daiem. He did his matriculation from Kurram Model High School Bannu. Then he admitted in Govt. degree college No. 2 Bannu from where he did his intermediate (pre-engineering) in 2001. Then he got admission in Govt. Post Graduate University Bannu and did his bachelor degree. Then he did his MSc Electronics from University of Peshwar. Presently he has awarded Scholarship form HEC for MS leading to PhD in Electronic Engineering.